

In presenting the dissertation as a partial fulfillment of the requirements for an advanced degree from the Georgia Institute of Technology, I agree that the Library of the Institute shall make it available for inspection and circulation in accordance with its regulations governing materials of this type. I agree that permission to copy from, or to publish from, this dissertation may be granted by the professor under whose direction it was written, or, in his absence, by the Dean of the Graduate Division when such copying or publication is solely for scholarly purposes and does not involve potential financial gain. It is understood that any copying from, or publication of, this dissertation which involves potential financial gain will not be allowed without written permission.

7/25/68

NUMERICAL MODELLING IN FLUID MECHANICS

A THESIS

Presented to

The Faculty of the Graduate Division

by

Bruce Ringsby Olmstead

In Partial Fulfillment

of the Requirements for the Degree

Master of Science in Civil Engineering

Georgia Institute of Technology

September, 1968

NUMERICAL MODELLING IN FLUID MECHANICS

Approved:

D. S.
Chairman: 21 50 14

10 1 0

Date Approved by Chairman: 9/23/68

ACKNOWLEDGMENTS

The author's gratitude is extended to all who helped to make this investigation possible. Special appreciation is extended to Dr. Paul G. Mayer for his interest, encouragement, guidance and patience during the preparation of this thesis. Dr. Mayer is also thanked for the author's introduction to this field of research, and the inspiration for many of the programs and examples selected.

The School of Civil Engineering is thanked for its support, both of the author and the research. Such support consisted of a NSF Traineeship, various assistantships and the provision of large amounts of computer time.

Appreciation is also extended to the staff of the Rich Electronic Computer Center for their efforts and patience with the author.

Gratitude is expressed to John M. Hamrick for assistance in the preparation of some of the programs, and to Professor G. D. May for his assistance in correcting the programs.

TABLE OF CONTENTS

| | Page |
|---|------|
| ACKNOWLEDGMENTS | ii |
| LIST OF FIGURES | iv |
| CHAPTER | |
| I. INTRODUCTION | 1 |
| II. MODELS AND TECHNIQUES IN ORDINARY DIFFERENTIAL EQUATIONS | 3 |
| III. DIFFERENCE SCHEMES IN PARTIAL DIFFERENTIAL EQUATIONS | 28 |
| IV. "FINITE ELEMENT" SCHEMES IN PARTIAL DIFFERENTIAL EQUATIONS | 48 |
| V. CONCLUSIONS | 72 |
| APPENDICES | |
| A. NOTATION | 74 |
| B. REFERENCES | 77 |

LIST OF FIGURES

| Figure | Page |
|---|------|
| 1. Pipe System for Example I | 10 |
| 2. Variation of Acceleration of Flow for Example I | 14 |
| 3. Variation in Flow Velocity, Example I | 15 |
| 4. Variation of Acceleration in Flow, Example II | 19 |
| 5. Variation in Velocity, Example II | 20 |
| 6. Graphical Representation of $T_1(x)$ | 26 |
| 7. Section of Grid | 30 |
| 8. Field for Example III | 31 |
| 9. Boundary Approximation | 33 |
| 10. Error Growth | 36 |
| 11. Domain of Dependence, Linear P and Q | 39 |
| 12. Pipe-Reservoir System | 43 |
| 13. Time Variation of Head at Valve, Example IV | 45 |
| 14. Water Depth over Pump Intake, Using Numerical Model of Example V | 47 |
| 15. Typical Element | 50 |
| 16. Normal Derivative | 54 |
| 17. Initial Solution Field for Example VI | 57 |
| 18. Free Surface as Computed for Example VI | 58 |
| 19. Axisymmetric Volume Element | 59 |
| 20. Thick-Walled Cylinder Modelled in Example VII | 63 |
| 21. Solution Field for Finite Element Model of Cylinder | 63 |

LIST OF FIGURES (Continued)

| Figure | Page |
|--|------|
| 22. Solution to Axisymmetric Heat Flow Problem (Example VII) | 65 |
| 23. Discretized Field for Solution of Transient Temperatures in Semi-Infinite Plate | 69 |
| 24. Transient Temperatures in Semi-Infinite Plate | 70 |

CHAPTER I

INTRODUCTION

The advent of the calculus and its subsequent development by Newton, Euler, Laplace and others has enabled the scientist and engineer to improve upon his algebraic analogues of the physical world by use of differential and integral equations. Though such models provide adequate descriptions in a conceptual sense, mathematical theory is often not sufficiently advanced to reduce the model to a closed-form analytic solution.

Such a gap has long existed; the evolution of mathematics and engineering science has advanced both solution techniques and scope of problems. The advent of high-speed computers has led to extensive use of numerical approximations to hitherto unsolvable problems, quite often with favorable results. Such numerical techniques usually have the effect of discretizing the solution field into elements for which an adequate solution is known or can be assumed. These elemental solutions are then joined to form an approximation to the actual solution. Ideally, such numerical techniques converge to the exact solution as the interval of discretization approaches zero.

Much common ground exists between the sundry techniques used in numerical modelling. Most methods rely upon the simulation of the unknown function by interpolational techniques (10),(15), or Taylor series. Oftentimes, final assembly of the elemental solutions draws upon the techniques of computational linear algebra (7),(9),(16),(12) these tools are not of immediate interest, and are well documented elsewhere. Of

more utility is the formulation and conception of various numerical techniques in the field of differential and integral equations, as these provide the basis for models of mathematical fluid mechanics.

In this thesis, a necessarily brief but representative review of current numerical methods is presented and examples illustrating applications to the mechanics of fluids are included. As a means to resolve some of the computational difficulties inherent in the application of older numerical techniques to the problems of fluid mechanics, recourse to the finite element method is made. This method, based upon Rayleigh-Ritz techniques, has been previously developed and is applied in its basic form to two-dimensional plane flow problems. In this thesis, the finite element method is extended to include formulations for axisymmetric and time-dependent problems. The Georgia Tech Rich Electronic Computer Center's Univac 1108 computer system has been used for the solution of the numerical examples.

CHAPTER II
MODELS AND TECHNIQUES IN ORDINARY
DIFFERENTIAL EQUATIONS

Lack of adequate mathematical theory and lack of mathematical skill have long frustrated engineers in the solution of engineering problems. Historically, such gaps have been bridged in part by the use of approximations based on experiments, and by the advent of the calculus which saw the same sort of approximations applied to its mathematical forms. In many instances, such approximations are no longer required today, although they may still represent relatively simple solutions for engineering purposes. In other cases, no adequate solution is known yet, providing impetus for further innovation in numerical approximations.

Approximate solution methods for ordinary differential equations usually fall into two general classes (2):

- I. A region of definition is assigned in advance over which an assumed solution is progressively evolved.
- II. A solution form, usually polynomial in nature, is assumed to be suitable for each relatively short interval. The parameters of such solution and the interval length are chosen so that the resulting solution is appreciably accurate.

Of the first class, the method most deserving of note is that due to M. Picard. In its classic form, Picard's method is used to obtain successive approximations to a solution of the equation

$$\frac{dy}{dx} = f(x, y(x)) . \quad (1)$$

With Picard's method, this equation is first transformed into the integral equation

$$y(x) = y_0 + \int_{x_0}^x f(x, y(x)) dx . \quad (2)$$

Starting with some functional approximation $y^{(0)}(x)$, an iteration is performed using

$$y^{(k)}(x) = y_0 + \int_{x_0}^x f(x, y^{(k)}(x)) dx . \quad (3)$$

Unfortunately, such integration is not easily done in general and numerical evaluation of a number of such integral approximations is time-consuming.

It has been suggested (14) that more practical use might be made of a modified Picard method.

Such modification permits the integration of an n^{th} -order differential equation

$$y^{(n)} = s_1(x)y^{(n-1)} + s_2(x)y^{(n-2)} + \dots + s_n(x)y + f(x) \quad (4)$$

where $s_i(x)$ are spatially varying coefficients for the derivative terms, and eliminates the necessity of the iterative solution when it is assumed that a uniform grid of size h is imposed upon the interval $[x_1, x_n]$. Then, equation (4) may be integrated as

$$\int_{x_0}^{x_1} y^{(n)} dx = \int_{x_0}^{x_1} \{ s_1(x) y^{(n-1)} + s_2(x) y^{(n-2)} + \dots + s_n(x) y + f(x) \} dx \quad (5)$$

or, under the assumption that $y^{(n)}$ is constant over the interval $[x_i, x_{i+1}]$.

$$y_{x_1}^{(n-1)} - y_{x_0}^{(n-1)} = h [s_1(x) y^{(n-1)} + \dots + s_n(x) y + f(x)] \quad (6)$$

Proceeding with successive terms

$$\int_{x_0}^{x_1} y_{x_1}^{(n-1)} dx = h y_{x_0}^{(n-1)} + \frac{h^2}{2} y_{x_0}^{(n)}$$

and in general,

$$\int_{x_0}^{x_1} y' dx = h y' + \frac{h^2}{2} y'' + \dots + \frac{h^n}{n!} y^{(n)} \quad (7)$$

When all terms of higher order than h are neglected, the formulation in matrix notation leads to

$$[D] = \begin{bmatrix} h s_1(x) & h s_2(x) & \dots & h s_n(x) \\ h & 0 & \dots & 0 \\ 0 & h & \dots & 0 \\ \dots & \dots & \dots & \dots \\ 0 & 0 & h & 0 \end{bmatrix} \quad (8)$$

$$y = \begin{Bmatrix} y^{(n-1)} \\ y^{(n-2)} \\ \vdots \\ y \end{Bmatrix}$$

and

$$\{y\}|_{x_1} = [D]\{y\}|_{x_0} + \{y\}|_{x_0} + hf(x)|_{x_0} \quad (9)$$

or,

$$\{y\}|_{x_1} = ([D] + [I])|_{x_0} \{y\}|_{x_0} + hf(x)|_{x_0} \quad (10)$$

$$\{y\}|_{x_2} = ([D] + [I])|_{x_1} \{y\}|_{x_1} + hf(x)|_{x_1} \quad (11)$$

or

$$\begin{aligned} \{y\}|_{x_2} = ([D] + [I])|_{x_1} ([D] + [I])|_{x_0} \{y\}|_{x_0} + ([D] + [I])hf(x)|_{x_0} \\ + hf(x)|_{x_1}. \end{aligned} \quad (12)$$

In general, this sequence becomes

$$\begin{aligned} \{y\}|_{x_k} = ([D] + [I])|_{x_{k-1}} \dots ([D] + [I])|_{x_0} \{y\}|_{x_0} + ([D] \\ + [I])|_{x_{k-1}} [hf|_{x_{k-2}} + ([D] + [I])|_{x_{k-2}} hf|_{x_{k-3}} + \dots] + hf|_{x_{k-1}} \end{aligned} \quad (13)$$

or,

$$\{y\}|_{x_k} = [F_k]\{y\}|_{x_0} + \text{vector depending upon } f(x) \text{ and } h. \quad (14)$$

The vector $\{y\}|_{x_k}$ may be thus easily computed from the known initial vector $\{y\}|_{x_0}$. This method also may be used to compute missing initial or final conditions by matrix manipulation, with known components

of $\{y\}|_{x_0}$ and $\{y\}|_{x_k}$, respectively.

The methods of the second class have as their basis that some polynomial or functional approximation is sufficiently accurate over some interval to satisfactorily approximate the solution to the differential equation. The size of such interval is generally left unspecified for derivational purposes, but is based upon permissible error in the approximate solution. Such methods usually are devised for the equation

$$y' = f(x, y) \quad (15)$$

$$y(x_0) = y_0$$

Among the most common solutions falling into this class is a series of solution formulae attributed to Runge and Kutta. Such Runge-Kutta procedures rely upon a linear approximation to the solution between the points y_i and $y_{(i+1)}$ with the reservation that a weighted slope is employed to determine the $(i+1)^{\text{st}}$ point. In such cases, it is desired to find the constants a, b, α, β so that

$$y_{i+1} = y_i + ak_1 + bk_2$$

$$k_1 = hf(x_i, y_i) \quad (16)$$

$$k_2 = hf(x_i + \alpha h, y_i + \beta k_1)$$

and agrees with a Taylor series approximation to the exact solution $\varphi(x)$ through powers of h as large as possible.

$$\varphi(x_{i+1}) = \varphi(x_i) + h\varphi'(x_i) + \frac{h^2}{2} \varphi''(x_i) + \frac{h^3}{3!} \varphi'''(x_i) + \frac{h^4}{4!} \varphi^{(iv)}(\xi_i) \quad (17)$$

where ξ_i is the point in $[x_i, x_{i+1}]$ where $\phi^{(iv)}(x)$ takes on a maximum,
or,

$$\begin{aligned} \phi(x_{i+1}) = \phi(x_i) + hf \frac{h^2}{2} \left[\frac{\partial f}{\partial x} + f \frac{\partial f}{\partial y} \right] \Big|_{x=x_i} + \frac{h^3}{6} \left[\frac{\partial^2 f}{\partial x^2} + 2f \frac{\partial^2 f}{\partial x \partial y} + \right. \\ \left. + f^2 \frac{\partial^2 f}{\partial y^2} + \frac{\partial f}{\partial x} \frac{\partial f}{\partial y} + f \left(\frac{\partial f}{\partial y} \right)^2 \right] \Big|_{x=x_i} + o(h^4) \end{aligned} \quad (18)$$

similarly,

$$\begin{aligned} \frac{k_2}{h} = f(x+ah, y+\beta k_1) = f(x_i, y_i) + ah \frac{\partial f}{\partial x} \Big|_{x=x_i} + \beta k_1 \frac{\partial f}{\partial y} \Big|_{x=x_i} + \quad (19) \\ + \frac{1}{2} \left[a^2 h^2 \frac{\partial^2 f}{\partial x^2} \Big|_{x=x_i} + 2ah\beta k_1 \frac{\partial^2 f}{\partial x \partial y} \Big|_{x=x_i} + \beta^2 k_1^2 \frac{\partial^2 f}{\partial y^2} \Big|_{x=x_i} \right] + o(h^3). \end{aligned}$$

Thus,

$$\begin{aligned} y_{i+1} = y_i + ahf(x_i, y_i) + bhf(x_i, y_i) + abh^2 \frac{\partial f}{\partial x} \Big|_{x=x_i} + \quad (20) \\ + h^2 \beta bf \frac{\partial f}{\partial y} \Big|_{x=x_i} + \frac{1}{2} \left[a^2 bh^3 \frac{\partial^2 f}{\partial x^2} \Big|_{x=x_i} + 2b\beta ah^3 f \frac{\partial^2 f}{\partial x \partial y} \Big|_{x=x_i} + \right. \\ \left. + \beta^2 bh^3 f^2 \frac{\partial^2 f}{\partial y^2} \Big|_{x=x_i} \right] + o(h^4) \end{aligned}$$

or,

$$\begin{aligned} y_{i+1} = y_i + h(a+b)f(x_i, y_i) + h^2 \left[ab \frac{\partial f}{\partial x} \Big|_{x=x_i} + \beta bf \frac{\partial f}{\partial y} \Big|_{x=x_i} \right] + \quad (21) \\ + h^3 \left[\frac{a^2 b}{2} \frac{\partial^2 f}{\partial x^2} \Big|_{x=x_i} + ba\beta f \frac{\partial^2 f}{\partial x \partial y} + b\beta^2 f^2 \frac{\partial^2 f}{\partial y^2} \Big|_{x=x_i} \right] + o(h^4) \end{aligned}$$

Comparing terms in equations (18) and (21), it is seen that

$$\begin{aligned} a + b &= 1 \\ \alpha b &= \frac{1}{2} \\ \beta b &= \frac{1}{2} . \end{aligned} \tag{22}$$

One solution for the system (22) is

$$\begin{aligned} a &= b = \frac{1}{2} \\ \alpha &= \beta = 1 . \end{aligned} \tag{23}$$

Thus, equations (16) become

$$\begin{aligned} y_{i+1} &= y_i + \frac{1}{2}(k_1 + k_2) \\ k_1 &= hf(x_i, y_i) \\ k_2 &= hf(x_i + h, y_i + k_1) . \end{aligned} \tag{24}$$

Here the error is $O(h^3)$.

By a similar but much lengthier development, it is seen that a higher-order solution to equations (15) takes the form

$$\begin{aligned} y_{i+1} &= y_i + \frac{1}{6}(k_1 + 2k_2 + 2k_3 + k_4) + O(h^5) \\ k_1 &= hf(x_i, y_i) \\ k_2 &= hf(x_i + \frac{1}{2}h, y_i + \frac{1}{2}k_1) \\ k_3 &= hf(x_i + \frac{1}{2}h, y_i + \frac{1}{2}k_2) \\ k_4 &= hf(x_i + h, y_i + k_3) . \end{aligned} \tag{25}$$

The use of this technique is demonstrated in Example I. This example also shows its application to systems of ordinary differential equations.

Example I

The distribution systems of water for a municipality is often subjected to large, rapidly-needed peak loads. One instance would be the rapid increase in flow required to meet the needs of fire-fighting in addition to the normal flow required through the distribution system. Current methods of meeting this demand are largely inadequate and expensive.

As an alternative to present methods, recent investigations suggested (15) that flow might be increased rapidly and cheaply by the addition of small amounts of drag-reducing polymer during periods of peak load. Such polymer additives are known to reduce resistance to flow by as much as 60%.

To predict possible flow patterns in a municipal water distribution system, a mathematical model to the situation must be formulated. For the purposes of this example, consider the elementary compound pipe system shown in Figure 1.

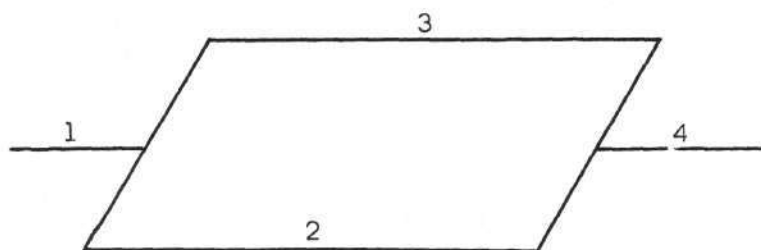


Figure 1. Pipe System for Example I.

This system has the following constants:

| Pipe | Length | Diam. | f Before | f After |
|------|--------|-------|----------|---------|
| 1 | 25.0' | 1.0' | 0.02 | 0.01 |
| 2 | 50.0' | .25' | 0.02 | 0.01 |
| 3 | 10.0' | .75' | 0.02 | 0.01 |
| 4 | 20.0' | 2.0' | 0.02 | 0.01 |

From mass and momentum balances (17),

$$V_1 D_1^2 = V_4 D_4^2 = D_2^2 V_2 + D_3^2 V_3 \quad (26)$$

$$x_i = \int_{t_0}^t V_i dt \quad (27)$$

$$\left(\frac{L_1}{g} \frac{D_2^2}{D_1^2} + \frac{L_2}{g} + \frac{L_4}{g} \frac{D_2^2}{D_4^2} \right) \frac{dV_2}{dt} + \left(\frac{L_1}{g} \frac{D_3^2}{D_1^2} + \frac{L_4}{g} \frac{D_3^2}{D_4^2} \right) \frac{dV_3}{dt} + \quad (28)$$

$$+ \frac{f_A L_1 + (f_B - f_A) x_1}{2g D_1} \frac{D_2^4}{D_1^4} + \frac{f_A L_2 + (f_B - f_A) x_1}{2g D_2} + \frac{f_A L_4 + (f_B - f_A) x_4}{2g D_4} \frac{D_2^4}{D_4^4} V_2^2 +$$

$$+ \frac{f_A L_1 + (f_B - f_A) x_1}{2g D_1} \frac{D_2^2}{D_1^2} \frac{D_3^2}{D_1^2} + \frac{f_A L_4 + (f_B - f_A) x_4}{g D_4} \frac{D_2^2 D_3^2}{D_4^4} V_2 V_3 +$$

$$+ \frac{f_A L_1 + (f_B - f_A) x_1}{2g D_1} \frac{D_3^4}{D_1^4} + \frac{f_A L_4 + (f_B - f_A) x_4}{g D_4} \frac{D_3^4}{D_4^4} V_3^2 = H_1 - H_4$$

$$\frac{L_2}{L_3} \frac{dV_2}{dt} - \frac{dV_3}{dt} + \frac{f_A L_2 + (f_B - f_A) x_2}{2L_3 D_2} V_2^2 - \frac{f_A L_3 + (f_B - f_A) x_3}{2L_3 D_3} V_3^2 = 0 \quad (29)$$

These equations thus are only a system of first-order ordinary differential equations in V_2 and V_3 , as

$$\frac{dV_2}{dt} = F_2(V_2, V_3, t) \quad (30)$$

$$\frac{dV_3}{dt} = F_3(V_2, V_3, t) \quad (31)$$

Applying Runge-Kutta procedures,

$$V_2^{(i+1)} = V_2^{(i)} + (k_1 + 2k_2 + 2k_3 + k_4)/6 \quad (32)$$

$$V_3^{(i+1)} = V_3^{(i)} + (K_1 + 2K_2 + 2K_3 + K_4)/6 \quad (33)$$

where

$$\begin{aligned} k_1 &= hF_2(V_2^{(i)}, V_3^{(i)}, t^{(i)}) \\ k_2 &= hF_2(V_2^{(i)} + \frac{1}{2} k_1, V_3^{(i)}, t^{(i)} + \frac{h}{2}) \\ k_3 &= hF_2(V_2^{(i)} + \frac{1}{2} k_2, V_3^{(i)}, t^{(i)} + \frac{h}{2}) \\ k_4 &= hF_2(V_2^{(i)} + k_3, V_3^{(i)}, t^{(i)} + h) \end{aligned} \quad (34)$$

and

$$\begin{aligned}
 K_1 &= hF_3(v_2^{(i)}, v_3^{(i)}, t^{(i)}) \\
 K_2 &= hF_3(v_2^{(i)}, v_3^{(i)} + \frac{1}{2} K_1, t^{(i)} + \frac{1}{2} h) \\
 K_3 &= hF_3(v_2^{(i)}, v_3^{(i)} + \frac{1}{2} K_2, t^{(i)} + \frac{1}{2} h) \\
 K_4 &= hF_3(v_2^{(i)}, v_3^{(i)} + K_3, t^{(i)} + h)
 \end{aligned} \tag{35}$$

The differential equations are thus solved in a step-by-step manner yielding the velocity and acceleration graphs shown in Figures 2 and 3.

Such methods as the Runge-Kutta procedures are dependent upon several calculations of functional values within the subinterval. For complicated functional expressions, this is a lengthy process at best. To simplify computational considerations, a somewhat different approach is employed in order to solve the system (15). One such multistep formula is the Adams-Bashforth method, which seeks to fit a 3rd degree interpolating polynomial to the known ordinates, and the next step is determined from this polynomial. The particular form of the interpolating polynomial used in this formulation is Newton's forward-difference interpolating polynomial,*

$$P_n(x) = f_0 + \sum_{j=1}^n \binom{s}{j} \Delta^j f_0 \tag{36}$$

Here $\binom{s}{j}$ denotes the binomial coefficients,

*Newton's forward-difference interpolating polynomial follows directly from the divided-difference form of the interpolating polynomial, as shown in Hildebrand (12).

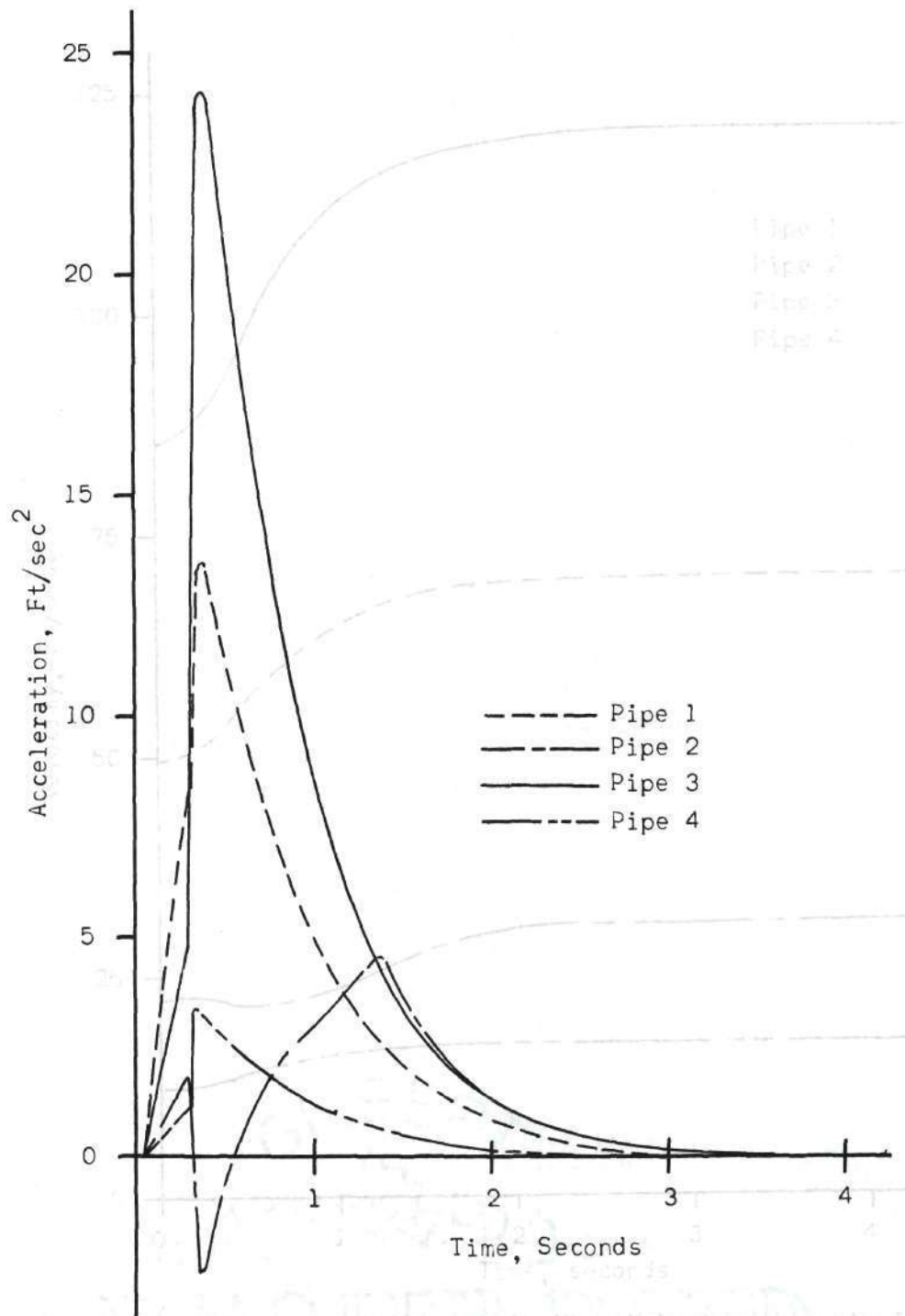


Figure 2. Variation in Acceleration of Flow for Example I.

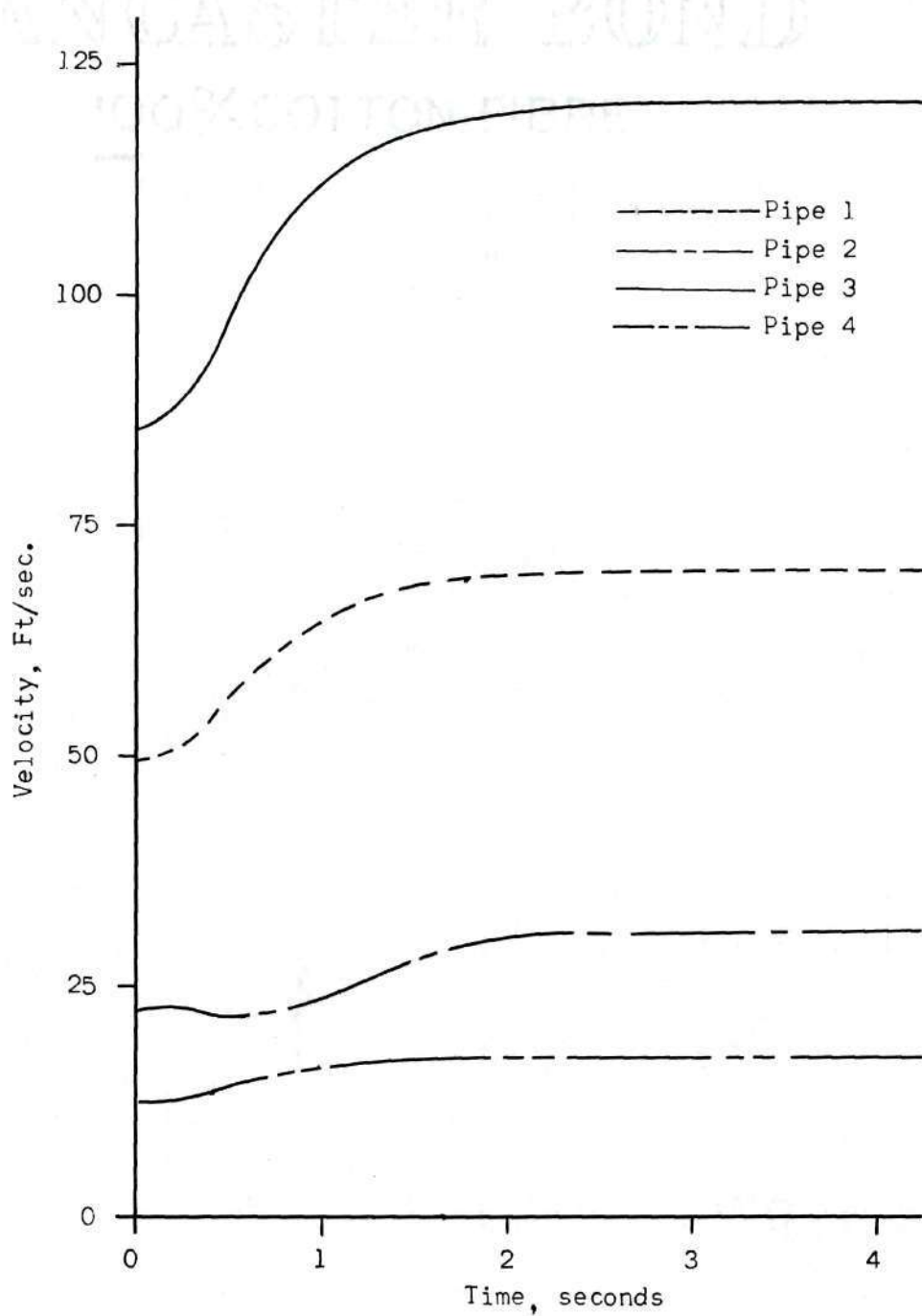


Figure 3. Variation in Flow Velocity, Example I.

s is defined by $x - x_i = (s-i)h$,

and

$$\begin{aligned}\Delta f_i &= f(x_{i+1}) - f(x_i) \\ \Delta^k f_i &= \Delta(\Delta^{k-1} f_i) .\end{aligned}\tag{37}$$

The Adams-Bashforth method, like Picard's method, begins not with the differential equation, but with an equivalent integral equation,

$$y_{i+1} = y_i + \int_{x_i}^{x_{i+1}} f[t, y(t)] dt \tag{38}$$

Equation (38) follows from equation (15). Here, $f(x, y)$ is approximated by an interpolating polynomial, equation (36), with the property that

$$f(x_j, y_j) = p_n(x_j) . \tag{39}$$

Placing this into (38)

$$y_{i+1} \approx y_i + \int_{x_i}^{x_{i+1}} p_n(x) dx . \tag{40}$$

Or,

$$y_{i+1} \approx y_i + \int_0^1 \sum_{j=0}^n (-1)^j \binom{-s}{jL} \Delta^j f_{i-k_j} h ds \tag{41}$$

and

$$y_{i+1} \approx y_i + \sum_{j=0}^n (-1)^j \Delta^j f_{i-j} h \int_0^1 \binom{-s}{L} ds \quad (42)$$

This is also expressed as

$$y_{i+1} \approx y_i + h(\gamma_0 f_i + \gamma_1 \Delta f_{i-1} + \dots + \gamma_n \Delta^n f_{i-1}) \quad (43)$$

from equation (42),

$$\gamma_k = (-1)^k \int_0^1 \binom{-s}{k} ds. \quad (44)$$

Carrying out the integration (44), it is seen that

$$\gamma_0 = 1$$

$$\gamma_1 = \frac{1}{2}$$

$$\gamma_2 = \frac{5}{12} \quad (45)$$

$$\gamma_3 = \frac{3}{8}$$

$$\gamma_4 = \frac{251}{720}$$

For the commonly used 3rd-degree polynomial, (43) becomes

$$y_{i+1} \approx y_i + h(f_i + \frac{1}{2} \Delta f_{i-1} + \frac{5}{12} \Delta^2 f_{i-2} + \frac{3}{8} \Delta^3 f_{i-3}) \quad (46)$$

or

$$y_{i+1} \approx y_i + h \left[f_i + \frac{1}{2}(f_i - f_{i-1}) + \frac{5}{12}(f_i - 2f_{i-1} + f_{i-2}) + \frac{3}{8}(f_i - 3f_{i-1} + 3f_{i-2} - f_{i-3}) \right] \quad (47)$$

which reduces to

$$y_{i+1} \approx y_i + \frac{h}{24} (55f_i - 59f_{i-1} + 37f_{i-2} - 9f_{i-3}) \quad (48)$$

Use of this technique is demonstrated in Example II.

Example II

In a similar view to that explored in Example I, the transient flow in a single pipe may be investigated by use of numerical techniques (15). As before momentum balance yields

$$\frac{L}{g} \frac{dV}{dt} + \frac{f_A L + (f_B - f_A)x}{2gD} V^2 = \Delta H \quad (49)$$

and

$$x = \int_{t_0}^t V dt. \quad (50)$$

For this problem, consider a pipe of the following dimensions:

$$L = 13.985 \text{ ft.}$$

$$D = 0.134 \text{ ft.}$$

$$f_A = 0.03$$

$$f_B = 0.015$$

$$\Delta H = 13.66 \text{ ft.}$$

Such model is solved using the Adams-Bashforth technique. Results are shown for velocity and acceleration in Figure 4 and 5.

As with the other methods, this method is only approximate, and the error present in each step (discretization error) may be found from

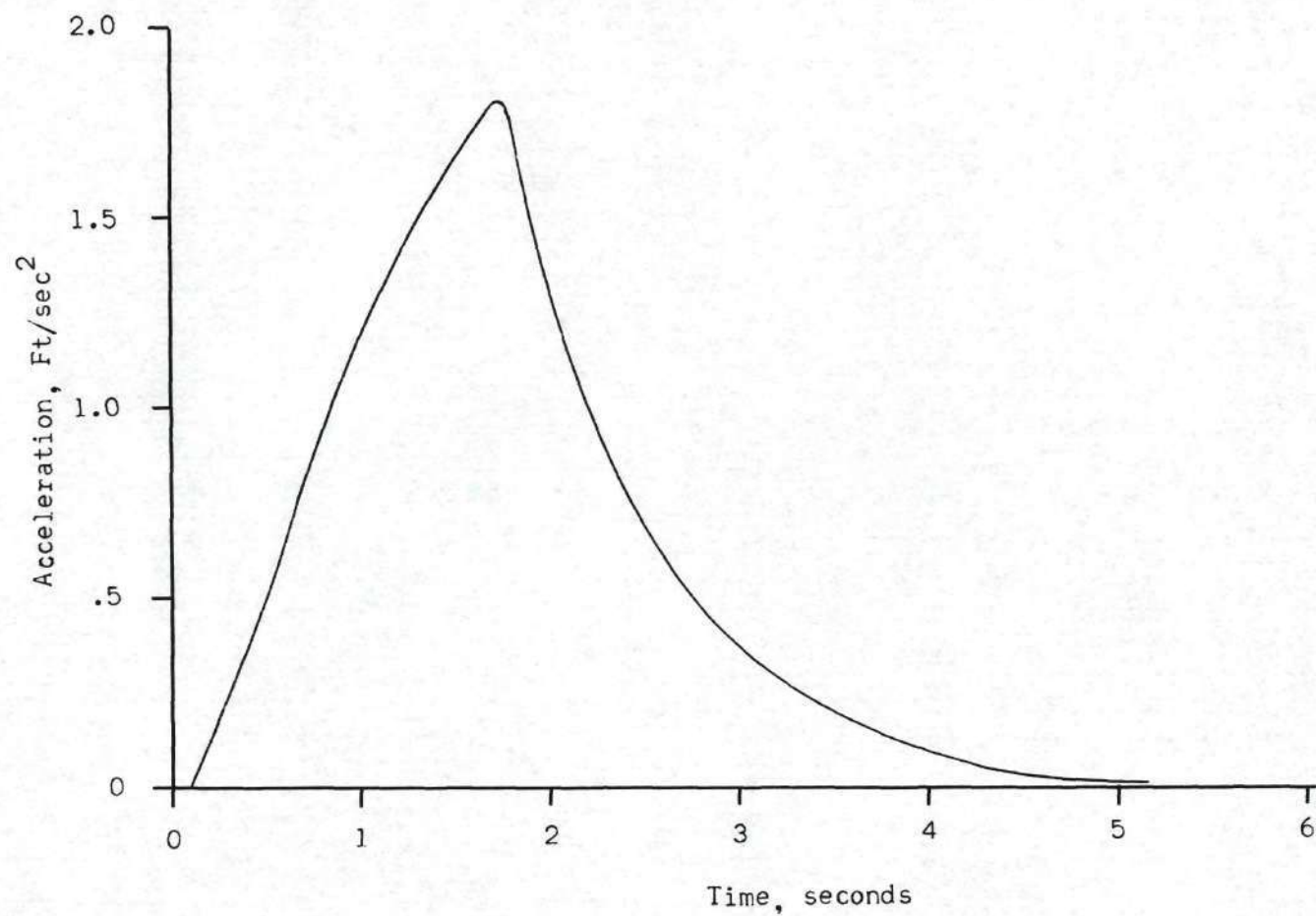


Figure 4. Variation of Acceleration in Flow, Example II.

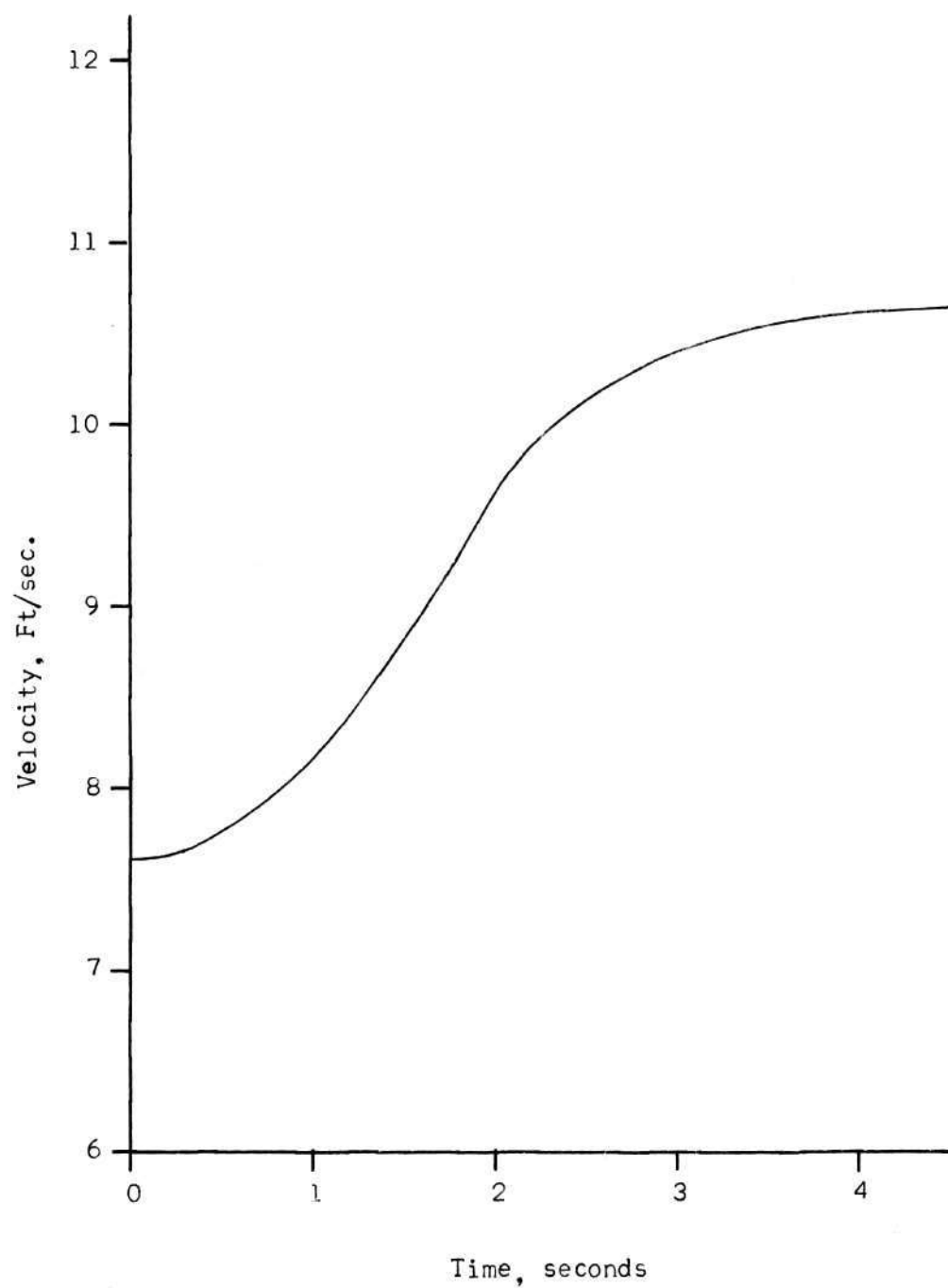


Figure 5. Variation in Velocity, Example II.

the error inherent in the interpolating polynomial from the divided-difference interpolating polynomial error term. If $P_3(x)$ is a third-degree polynomial,

$$R(x) = \frac{(x-x_i)(x-x_{i-1})(x-x_{i-2})(x-x_{i-3})}{(4!)} f^{(iv)}(n, \varphi(\eta)) . \quad (51)$$

The step-by-step error thus becomes

$$E = \int_{x_i}^{x_{i+1}} R(x) dx = h^5 \int_0^1 \binom{-s}{4} f^{(4)}(n, \varphi(\eta)) ds \quad (52)$$

or,

$$E = \frac{251}{720} h^5 f^{(iv)}(\eta) . \quad (53)$$

Even though such methods as the Adams-Bashforth routine outlined here entail relatively less computational effort than the Runge-Kutta procedures, they still represent a compromise of sorts. This is because they are not self-starting, i.e., they need 4 previously-computed points from which to begin the solution. These are usually determined by use of a Runge-Kutta routine. In addition, such multistep methods require that a constant step size be used for the solution. This requirement is not necessary for the Runge-Kutta procedures.

The extension of either case discussed above to systems of such equations is obvious. In each instance, all pertinent information is known at the i^{th} previous points, and solution is desired for the $(i+1)^{\text{st}}$ point. With this in mind, it is seen that each of the equations of a linear system may be solved as though it were by itself. Reference to

Example I provides an illustration of the technique.

Similarly, an extension to higher-order equations may be accomplished through a substitution for lower-order derivatives. Such result is a linear system of first-order equations, which solution has been discussed.

Theoretically the error in such step-by-step integration of a differential equation may be viewed as a contribution both from the roundoff error and truncation error. From a computational point of view, analysis of such error is perhaps difficult, if conducted on other than an order-of-magnitude basis. This difficulty is encountered in both types of error; in the case of roundoff error, a statistical approximation to error bounds is difficult to use, and analysis of truncation error results at times in poorly specified quantities. Thus, commonly, only an order-of-magnitude error analysis is employed.

As is noted from equation (15), the methods discussed thus far are applicable (with one exception) only to initial (or final) value problems. For a 1st-order equation, this represents virtually the only possibility. For higher-order equations it does not. Rather, such higher-order equations are often boundary-value problems, and as such are difficult, if not impossible to solve with the previously mentioned methods.

Classically, such problems are approached by means of a finite-difference scheme. To see how such a scheme might work, consider the problem

$$-\frac{d^2y}{dx^2} + r(x)y(x) = f(x) \quad (54)$$

$$y(a) = \alpha$$

$$y(b) = \beta$$

for the interval $[a, b]$. The interval $[a, b]$ is divided into N subintervals of length h . Approximation of $y(x)$ by parabolic interpolation and differentiation of the resulting polynomial yields

$$\left. \frac{d^2 y}{dx^2} \right|_{x=x_i} = \frac{y_{i+1} - 2y_i + y_{i-1}}{h^2} - \frac{h^2}{12} y^{(iv)}(\xi) \quad (55)$$

Substituted into (54), this becomes

$$\frac{2y_i - y_{i+1} - y_{i-1}}{h^2} + r_i y_i = f_i \quad (56)$$

$$y_0 = \alpha$$

$$y_{N+1} = \beta$$

The result is thus N equations in N unknowns, as

$$[A]\{y\} = \{b\} + \{e(y)\} \quad (57)$$

where

$$[A] = \frac{1}{h^2} \begin{bmatrix} 2+r_1 h^2 & -1 & 0 & \dots & 0 \\ -1 & 2+r_2 h^2 & -1 & \dots & 0 \\ 0 & -1 & 2+r_3 h^2 & \dots & 0 \\ \dots & \dots & \dots & \dots & \dots \\ 0 & 0 & 0 & \dots & 2+r_n h^2 \end{bmatrix} \quad (58)$$

and

$$b = \begin{Bmatrix} f_1 + \frac{\alpha}{h^2} \\ f_2 \\ f_3 \\ \vdots \\ f_n + \frac{\beta}{h^2} \end{Bmatrix} \quad (59)$$

The error vector $\{e(y)\}$ is ignored, and the solution to (54) is approximated by

$$[A]\{y\} = \{b\} . \quad (60)$$

Equation (60) may then be solved using the techniques outlined in Faddeeva (12). For the particular case of a tridiagonal system as (58), formulae derived using Gaussian reduction (7) are recommended.

All the methods discussed thus far are alike in that they search for an approximate solution to an exact functional relationship while such approach is valid in itself. It is, however, not the only way. An alternative approach is to recognize that any mathematical solution is at best approximate, and rather than approximate a solution, the function itself is approximated. Such method is the Rayleigh-Ritz procedure.

For illustrative purposes the solution to equation (54),

$$-y'' + r(x)y(x) = f(x)$$

$$y(a) = \alpha$$

$$y(b) = \beta$$

is formulated in this manner. For simplicity's sake, consider the interval $[a, b]$ subdivided into N subintervals of equal length h . This done, it can be shown that equivalent to a solution of (54) is some function $u(x)$ which makes

$$I = \int_a^b \left\{ \frac{1}{2} \left(\frac{du}{dx} \right)^2 + \frac{1}{2} r(x) u^2(x) - u(x) f(x) \right\} dx \quad (61)$$

a minimum. For a physical interpretation, equation (61) may be regarded as a representation of the energy of a physical system. The principle of minimum energy would require that I be minimum, if $u(x)$ were indeed characteristic to that system.

The form of the approximate function is now selected; its only constraint is that it must be piecewise continuous. For simplicity, a linear form

$$u(x) = u_i + \frac{u_{i+1} - u_i}{h} (x - x_i), \quad (x_i < x < x_{i+1}) \quad (62)$$

is chosen. Note also that

$$u'(x) = \frac{u_{i+1} - u_i}{h}, \quad (x_i < x < x_{i+1}). \quad (63)$$

Equation (61) thus becomes

$$I = \sum_{i=0}^N \int_{x_i}^{x_{i+1}} \left\{ \frac{1}{2} \left(\frac{u_{i+1} - u_i}{h} \right)^2 + \frac{1}{2} r(x) \left[u_i + \frac{u_{i+1} - u_i}{h} (x - x_i) \right]^2 - \left[u_i + \frac{u_{i+1} - u_i}{h} (x - x_i) \right] f(x) \right\} dx. \quad (64)$$

Equation (64) is then minimized with respect to u_i .

$$\begin{aligned} \frac{\partial I}{\partial u_i} = & \int_{x_{i-1}}^{x_i} \left\{ \frac{1}{h} \left(\frac{u_i - u_{i-1}}{h} \right) + r(x)u(x) \left[\frac{1}{h}(x - x_{i-1}) - \frac{1}{h}[x - x_i] \right] f(x) \right\} dx + \quad (65) \\ & + \int_{x_i}^{x_{i+1}} \left\{ -\frac{1}{h} \left(\frac{u_{i+1} - u_i}{h} \right) + r(x)u(x) \left[1 - \frac{x - x_i}{h} \right] - f(x) \right. \\ & \left. + \frac{x - x_i}{h} f(x) \right\} dx = 0 \end{aligned}$$

or,

$$\frac{u_i - u_{i-1}}{h} + \frac{u_i - u_{i+1}}{h} + \int_{x_{i-1}}^{x_{i+1}} r(x)u(x)T_i(x)dx - \int_{x_{i-1}}^{x_{i+1}} f(x)T_i(x)dx = 0 \quad (66)$$

where $T_i(x)$ is shown graphically below.

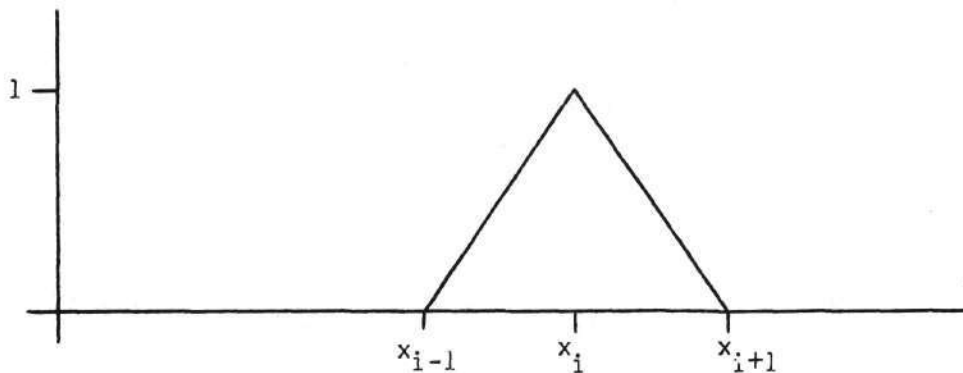


Figure 6. Graphical Representation of $T_i(x)$.

More simply,

$$\frac{-u_{i+1} + 2u_i - u_{i-1}}{h} + \int_{x_{i-1}}^{x_{i+1}} r(x)u(x)T_i(x)dx = \int_{x_{i-1}}^{x_{i+1}} f(x)T_i(x)dx \quad (67)$$

With $f(x)$ and $r(x)$ specified, equation (67) is integrated over the interval $[a,b]$ to yield an $N \times N$ system of the form

$$[A]\{u\} = \{b\} \quad (68)$$

by means of which values of u_i are obtained. Such methods also serve for solution of partial differential equations of certain types, as will be discussed in due course.

CHAPTER III

DIFFERENCE SCHEMES IN PARTIAL DIFFERENTIAL EQUATIONS

The advent of high-speed digital computing machinery has vastly increased the use of approximate numerical methods in the solution of partial differential equations for the evaluation of associated mathematical models. Problems involving such solutions, as well as methods of solution, are virtually boundless, thus rendering a completely general discussion difficult. Looking towards applicability to the mechanics of fluids, it is possible to limit the discussion. This does, however, not limit the generality of methods discussed.

Spurred by the lack of a complete theoretical understanding of the solution to partial differential equations, it is common practice to attempt to reduce the partial differential equation to equivalent ordinary differential equations (11). Such methods are of particular applicability when the problem is concerned with an easily-defined field. In many cases, numerous transformations are required to reduce the problem to an amenable form. The resulting ordinary differential equations are then solved either numerically or analytically.

Requisite of such techniques is that they be applied to easily-defined fields, and that associated boundary conditions also be easily defined. In many problems this condition is not satisfied, and recourse must be made to other methods, often involving considerably more conceptual complexity. In addition, some equations are not amenable to reduction to ordinary differential equations. Such cases require obviously

more ingenious approaches to their solution.

Such methods are by no means new (3). Bernoulli, Euler, and others made extensive use of difference equations in early investigations of physical phenomena. It was, however, well into the current century before numerical techniques found wide acceptance by the engineering profession (19).

The basis of difference formulations lies in an assumed functional relationship over all or over a portion of the field under consideration. Generally, the relationship is an interpolating polynomial of some sort, the parabola being common for most second-order applications. Differentiation of such forms at known points yields simple difference approximations to the derivative; combinations of such forms may be used to approximate the differential equation at a point. Lines along which the interpolating polynomial is formed are defined by superposing a grid of sufficient fineness upon the region under consideration. The solution to the boundary value problem is approximated by the computed functional values at the intersections of the grid lines.

To amplify upon such approximation, consider the portion of the grid shown by Figure 7, and the equation $\frac{\partial^2 u}{\partial x^2} + \frac{\partial^2 y}{\partial y^2} = 0$.

From the differentiation of a parabolic interpolating polynomial, it is seen that

$$\left. \frac{\partial^2 y}{\partial x^2} \right|_{\substack{x=x_i \\ y=y_i}} = \frac{u_{i,j+1} - 2u_{i,j} + u_{i,j-1}}{h^2} - \frac{h^2}{12} u^{(iv)}(\xi_1) \quad (69)$$

and

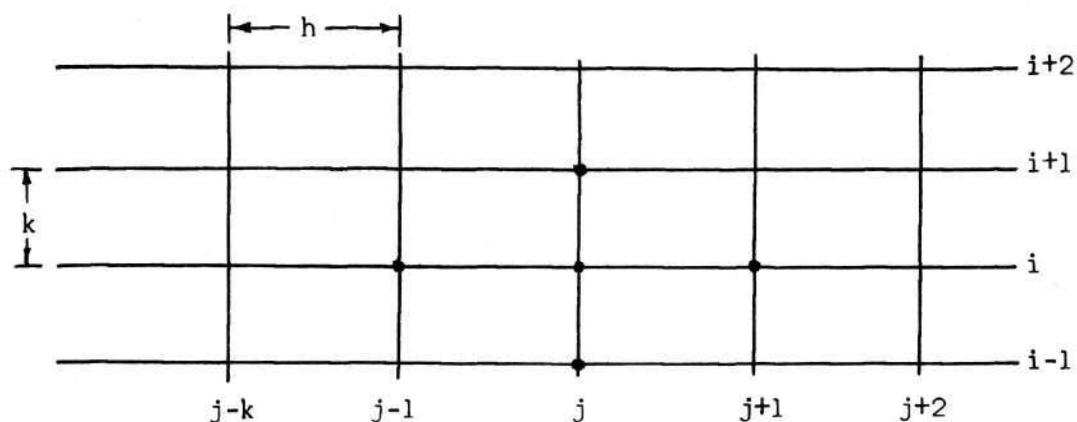


Figure 7. Section of Grid.

$$\left. \frac{\partial^2 u}{\partial y^2} \right|_{\substack{x=x_i \\ y=y_i}} = \frac{u_{i+1,j} - 2u_{i,j} + u_{i-1,j}}{k^2} - \frac{k^2}{12} u^{(iv)}(\xi_2) \quad (70)$$

Combining equations (65) and (70) and neglecting the error terms, Laplace's equation is approximated at point x_j, y_i by

$$\frac{u_{i,j+1} - 2u_{i,j} + u_{i,j-1}}{h^2} + \frac{u_{i+1,j} - 2u_{i,j} + u_{i-1,j}}{k^2} = 0 \quad (71)$$

As the indices i and j change over the region, an equation of the form of (71) is set up for each point x_j, y_i , and a set of homogeneous simultaneous equations results that approximates the portion of the field under consideration.

Just as with the partial differential equation, a unique solution here depends upon the boundary conditions imposed upon the field. Boundary conditions, as used with the difference equation (71), are subtracted from both sides of the resulting homogeneous system, rendering the system

amenable to a unique solution.

To illustrate how such a boundary value problem might be set up for solution, consider Example III.

Example III

$$\begin{aligned}\frac{\partial^2 u}{\partial x^2} + \frac{\partial^2 u}{\partial y^2} &= 0 \quad 0 \leq x, y \leq 1 \\ u(0, y) &= u(1, y) = 9y^2 \\ y(x, 0) &= 0 \\ u(x, 1) &= 9\end{aligned}\tag{72}$$

The field under consideration here is the unit square, and for the purposes of this illustration may be considered to be represented by the mesh shown in Figure 8.

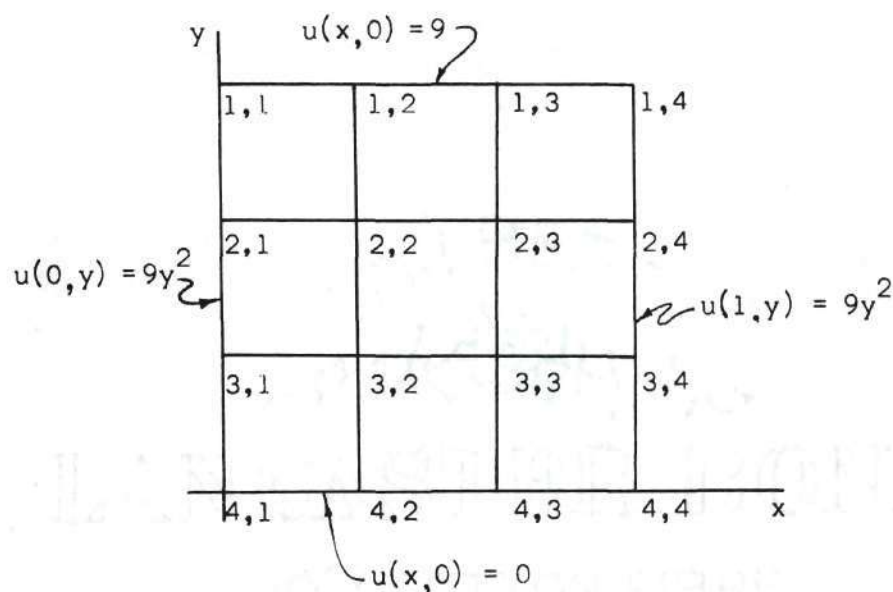


Figure 8. Field for Example III.

In this illustration, boundary points are known; a solution is needed only for interior points. Using a twice-differentiated interpolating polynomial, with grid spacing equal in each direction, the difference approximation to (72) becomes

$$\frac{u_{i+1,j} - 2u_{i,j} + u_{i-1,j}}{h^2} + \frac{u_{i,j+1} - 2u_{i,j} + u_{i,j-1}}{h^2} = 0 \quad (73)$$

or

$$-u_{i+1,j} - u_{i-1,j} - u_{i,j+1} - u_{i,j-1} + 4u_{i,j} = 0 \quad (74)$$

Using equation (74), the system describing $u(x,y)$ at the interior nodes becomes

$$\begin{bmatrix} +4 & -1 & -1 & 0 \\ -1 & 4 & 0 & -1 \\ -1 & 0 & 4 & -1 \\ 0 & -1 & -1 & 4 \end{bmatrix} \begin{Bmatrix} u_{2,2} \\ u_{2,3} \\ u_{3,2} \\ u_{3,3} \end{Bmatrix} = \begin{Bmatrix} 13 \\ 13 \\ 1 \\ 1 \end{Bmatrix} \quad (75)$$

The system (75) is then solved using pertinent methods of computational linear algebra.

Most commonly used of such techniques are the iterative solutions: Point-Jacobi, Gauss-Seidel, or successive over-relaxation. Written in the form for solution by for instance the Point-Jacobi Iteration, the interior points are determined by

$$u_{i,j}^{(k+1)} = \frac{1}{4} [u_{i+1,j}^{(k)} + u_{i-1,j}^{(k)} + u_{i,j+1}^{(k)} + u_{i,j-1}^{(k)}] \quad (76)$$

it has been shown (23) that such a formulation as (76) will, indeed con-

verge to the solution of Laplace's equation.

Difference approximations to the solutions of partial differential equations, such as the approximation outlined in Example III for Laplace's equation are by nature best suited to rectangular fields. In many engineering applications, however, it is difficult if not impossible to reduce the problem to such form. Consequently, various methods (16) are suggested for the modification of the difference approximation in order that the shape and geometrical properties of the problem might be adequately represented. If used with hand computation methods, such as a desk calculator, such formulations along a boundary may be used with little additional effort. Digital computer application of difference schemes virtually precludes the use of such boundary point formulae, due to programming difficulties. For such application, it is usually sufficient to assume an approximate boundary form, which is composed of nodes still located at the normal grid interval, as shown in Figure 9.

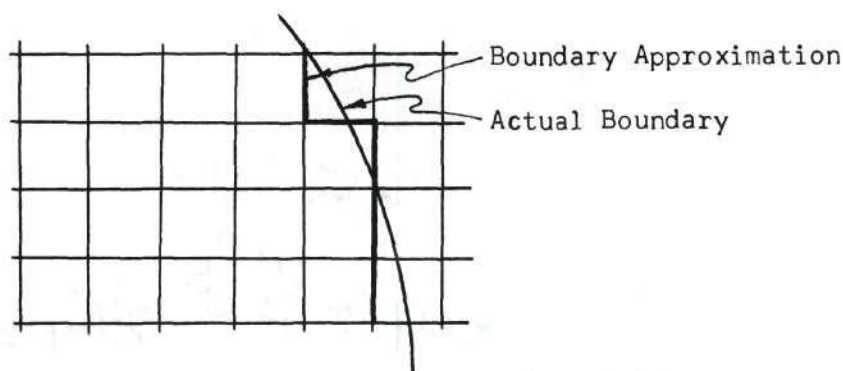


Figure 9. Boundary Approximation.

In addition to specified boundary values, the solution to many problems

hinges upon the values of normal derivatives along portions of the boundary. In such cases, these boundary conditions are also written in difference form, making use of either "image points" outside the boundary, or non-symmetric differences within the boundary. The above methods are treated in great depth by Southwell and Allen (1),(23),(24).

Unspecified boundary geometry associated with fields encountered in many hydraulic engineering applications has led to various transformations to reduce the problem at hand to a geometry more amenable to solution (6),(17). This newly-defined region is then solved using difference techniques and transformed back to the original plane. Such methods have been applied effectively to free-streamline application in inviscid or potential flow problems. Numerical examples are given in (6) and (17).

Equations of the elliptic type, as discussed above do not represent the only application of difference approximations in the solution of partial differential equations. As another instance, parabolic equations of the form

$$\frac{\partial u}{\partial t} = c^2 \frac{\partial^2 u}{\partial x^2} \quad (77)$$

are also approximated by the solution of an associated difference equation. In such application, however, the solution is a step-by-step solution in t , and care must be taken as to the difference approximation used and the grid spacing. If such is not done, the equation will be unstable, and results in a rapid growth of error (26).

Computational schemes which work quite well make use of difference approximations involving different orders of error for a solution in x

and t . This necessitates different step size in either direction. To elucidate, consider the problem below:

$$\frac{\partial u}{\partial t} = r^2 \frac{\partial^2 u}{\partial x^2} \quad (78)$$

$$u(a) = \alpha, \quad u(b) = \beta$$

$$u(0, x) = u_0$$

The second-derivative term is approximated as in the previous elliptic examples. For the derivative in t , however, a central-difference scheme is unstable; forward or backward differences must be used. For the purposes of illustration, forward differences are employed.

In approximating such a solution, the difference equations may be considered to be solved along a grid system in the x - t plane. This grid is of spacing h in the x -direction and spacing k in the t -direction. Here h and k need not be equal.

Using such a difference scheme, equation (78) becomes

$$\frac{u_{i,j+1} - u_{i,j}}{k} = r^2 \frac{u_{i+1,j} - 2u_{i,j} + u_{i-1,j}}{h^2} \quad (79)$$

or

$$u_{i,j+1} = \frac{r^2 k}{h^2} u_{i+1,j} + \left(1 - \frac{2r^2 k}{h^2}\right) u_{i,j} + \frac{r^2 k}{h^2} u_{i-1,j} \quad (80)$$

A relationship between h and k are best established by an examination of the growth a small error of size ϵ as a solution involving equation (80) proceeds. Such solution is shown in Figure 10. Instability

$$\begin{array}{cccccc}
 + & & + & & + & & + & & + & & + \\
 & & & & (1 - 4 \frac{r^2 k}{h^2} + \frac{6r^4 k^2}{h^4}) \epsilon & & & & & & \\
 + & & + & & + & & + & & + & & + \\
 \frac{r^4 k^2}{h^4} \epsilon & (1 - 2 \frac{r^2 k}{h^4}) \frac{r^2 k}{h^2} \epsilon & & & (1 - 2 \frac{r^2 k}{h^4}) \frac{r^2 k}{h^2} \epsilon & & & & \frac{r^4 k^2}{h^4} \epsilon & & \\
 + & & + & & + & & + & & + & & + \\
 & & \frac{r^2 k}{h^2} & & (1 - 2 \frac{r^2 k}{h^2}) \epsilon & & \frac{r^2 k}{h^2} \epsilon & & & & \\
 + & & + & & + & & + & & + & & + \\
 & & & & \epsilon & & & & & &
 \end{array}$$

Figure 10. Error Growth.

in such a solution depends solely upon the size of the parameter $r^2 k / h^2$. From Figure 10, it is seen that for $2 \frac{r^2 k}{h^2} < 1$, the error ϵ is damped out as the solution proceeds. Thus for good solution using the scheme outlined by equation (85), h and k must be determined so that $\frac{h^2}{k} \leq 2r^2$.

Boundary conditions for these difference relations are inserted as the $(i \pm 1)^{\text{st}}$ term in the difference relation, as such terms are encountered. If, for an alternative case, normal derivative boundary conditions are given, an additional equation and possibly image points would be used, as in the previous discussion of boundary conditions. Southwell (23), (24) illustrates such methods.

The treatment of hyperbolic equations by difference techniques is also possible though still subject to constraints. Equations of this sort are represented by a form

$$\frac{\partial^2 u}{\partial t^2} = r^2 \frac{\partial^2 u}{\partial x^2} \quad (81)$$

$$u(x, 0) = g(x) \quad -\infty < x < \infty$$

$$\frac{\partial u}{\partial t}(x, 0) = f(x)$$

Such an equation has a mathematically concise form for its solution. As may be verified by substitution, the solution is

$$u(x, t) = P(x + \gamma t) + Q(x - \gamma t) \quad (82)$$

where P and Q must be twice-differentiable functions. Though mathematically correct, such form is not sufficiently precise for computational utility. To see what form the solution takes on, an investigation of P and Q is advisable.

It is known that P and Q must satisfy

$$u(x, t) = P(x + \gamma t) + Q(x - \gamma t) \quad (83)$$

$$u(x, 0) = P(x) + Q(x) = g(x)$$

$$\frac{\partial u}{\partial t}(x, 0) = \gamma P'(x) - \gamma Q'(x) = f(x)$$

From equations (83)

$$P'(x) - Q'(x) = \frac{1}{\gamma} f(x) \quad (84)$$

Integrating from 0 to $x + \gamma t$

$$P(x) - P(0) - Q(x) + Q(0) = \frac{1}{\gamma} \int_0^x f(\xi) d\xi \quad (85)$$

or,

$$P(x) - Q(x) = \frac{1}{\gamma} \int_0^x f(\xi) d\xi + P(0) - Q(0) \quad (86)$$

$$P(x) + Q(x) = g(x)$$

Thus

$$P(x) = \frac{1}{2} g(x) + \frac{1}{2\gamma} \int_0^x f(\xi) d\xi + \frac{1}{2} P(0) - Q(0) \quad (87)$$

and

$$Q(x) = \frac{1}{2} g(x) - \frac{1}{2\gamma} \int_0^x f(\xi) d\xi - \frac{1}{2} P(0) - Q(0) \quad (88)$$

or, by analogy

$$u(x,t) = \frac{1}{2} g(x+\gamma t) + g(x-\gamma t) + \frac{1}{2\gamma} \int_{x-\gamma t}^{x+\gamma t} f(\xi) d\xi. \quad (89)$$

Insofar as computational utility is concerned equation (89) represents no distinct advantage, but it does yield information as to the domain that such solution for $u(x,t)$ must encompass. That is, $u(x,t)$ depends only upon values of x lying in the interval $[x-\gamma t, x+\gamma t]$. If, for example, $P(x+\gamma t)$ and $Q(x-\gamma t)$ were linear, the domain of dependence for $u(x,t)$ would be the shaded area shown in Figure 11.

In order that a numerical model approximating equation (81) be appropriate, the model must also encompass this domain of dependence. The lack of such condition is indicated by instability in similar fashion to that of the parabolic equation shown in Figure 10.

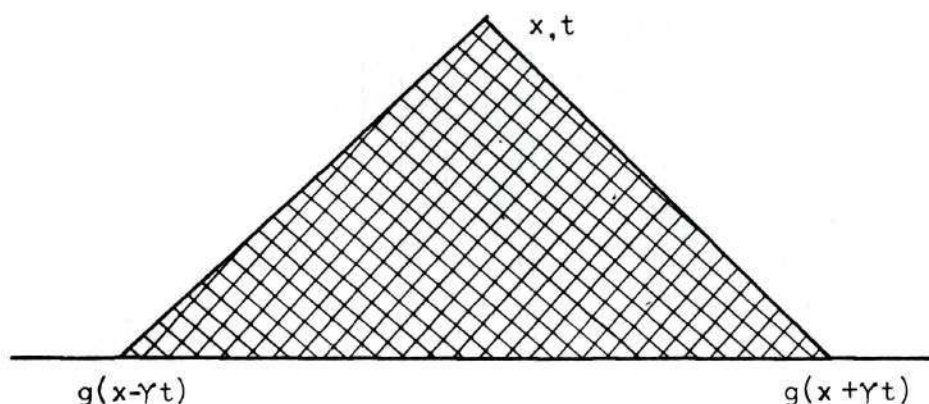


Figure 11. Domain of Dependence, Linear P and Q.

A numerical model for such a problem is set up on a grid system in an x - t plane, with a grid spacing of k along the t -direction and spacing h along the x -axis. k and h need not be equal, and in order to satisfy the condition that such a numerical model encompass the domain of dependence of the differential equation, the spacing must obey the relation

$$\frac{k}{h} \leq \frac{1}{\gamma} \quad (90)$$

With this in mind, equations (81) may be approximated by

$$\frac{u_{i,j+1} - 2u_{i,j} + u_{i,j-1}}{k^2} - \gamma^2 \frac{u_{i+1,j} - 2u_{i,j} + u_{i-1,j}}{h^2} = 0 \quad (91)$$

or

$$u_{i,j+1} = \frac{\gamma^2 k^2}{h^2} [u_{i+1,j} - 2u_{i,j} + u_{i-1,j}] + 2u_{i,j} - u_{i,j-1} \quad (92)$$

and the derivative boundary conditions are specified either by Taylor series or by unsymmetrical differences.

A more common solution method reduces equation (81) to the equivalent problem

$$\frac{\partial u}{\partial t} = \gamma_1 \frac{\partial v}{\partial x} \quad (93)$$

$$\frac{\partial v}{\partial t} = \gamma_2 \frac{\partial u}{\partial x}$$

$$u(x, 0) = g(x)$$

$$v(x, 0) = G(x)$$

The grid spacing for these equations is subject to the same criterion as for equation (81). Subsequently, a linear combination of the system (93) is solved for u , v , x , and t .

In the instance above, using Lagrange multipliers,

$$\frac{\partial u}{\partial t} - \gamma_1 \frac{\partial v}{\partial x} + \lambda \frac{\partial v}{\partial t} - \lambda \gamma_2 \frac{\partial u}{\partial x} = 0 \quad (94)$$

or

$$\frac{\partial u}{\partial t} - \gamma_2 \lambda \frac{\partial u}{\partial x} + \lambda \frac{\partial v}{\partial t} - \frac{\gamma_1}{\lambda} \frac{\partial v}{\partial x} = 0. \quad (95)$$

Each term reduces to a total differential if

$$\frac{dx}{dt} = \gamma_2 \lambda = + \frac{\gamma_1}{\lambda} \quad (96)$$

or,

$$\lambda = \pm \sqrt{\frac{\gamma_1}{\gamma_2}} \quad (97)$$

and

$$\frac{dx}{dt} = \pm \sqrt{\gamma_1 \gamma_2} \quad (98)$$

The system to be solved then becomes

$$\frac{du}{dt} \pm \sqrt{\gamma_1 \gamma_2} \frac{dv}{dt} = 0 \quad (99)$$

$$\frac{dx}{dt} = \pm \sqrt{\gamma_1 \gamma_2}$$

Applying backward or forward differences as applicable to equations (99). Four simultaneous algebraic equations in u , v , x , and t result. Such solution is demonstrated in Examples IV and V.

Example IV

The conception of large hydroelectric facilities often involves the design of long penstocks between the reservoir and the turbine facility. For such long conduits, it becomes critical that transient effects associated with the operation of values be investigated.

The formulation of an analytic technique begins with balance equations for mass and momentum. These equations are then reduced to the wave equation

$$\frac{\partial^2 H}{\partial t^2} = a^2 \frac{\partial^2 H}{\partial x^2} \quad (100)$$

or the two associated linear differential equations:

$$\frac{\partial v}{\partial x} + \frac{g}{a^2} \frac{\partial H}{\partial t} = 0 \quad (101)$$

and

$$g \frac{\partial H}{\partial x} + \frac{\partial V}{\partial t} + \frac{f}{2D} V|V| = 0 . \quad (102)$$

Here, f is the Darcy-Weisbach friction factor.

These equations may be combined by the use of a Lagrangian multiplier as

$$\lambda \frac{dH}{dt} + \frac{dV}{dt} + \frac{fV|V|}{2D} = 0 \quad (103)$$

and

$$\frac{dx}{dt} = \frac{g}{\lambda} \quad (104)$$

where

$$\lambda = \pm \frac{g}{a} \quad (105)$$

This results in four ordinary differential equations

$$\frac{g}{a} \frac{dH}{dt} + \frac{dV}{dt} + \frac{fV|V|}{2D} = 0 \quad (106)$$

$$\frac{dx}{dt} = + a \quad (107)$$

$$- \frac{g}{a} \frac{dH}{dt} + \frac{dV}{dt} + \frac{fV|V|}{2D} = 0 . \quad (108)$$

$$\frac{dx}{dt} = -a \quad (109)$$

Backwards and forward differences are applied to these equations, yielding

$$\frac{g}{a} (H_i - H_{i-1}) + (V_i - V_{i-1}) + \frac{fV|V|}{2D} \Big|_{i-1} \Delta t = 0 \quad (110)$$

$$x_i - x_{i-1} = a\Delta t \quad (111)$$

$$-\frac{g}{a} (H_i - H_{i+1}) + (V_i - V_{i+1}) + \frac{fV|V|}{2D} \Big|_{i+1} \Delta t = 0 \quad (112)$$

$$x_i - x_{i+1} = a\Delta t \quad (113)$$

This technique was programmed for the Burroughs B-5500 computer system and used to solve the system shown in Figure 12.

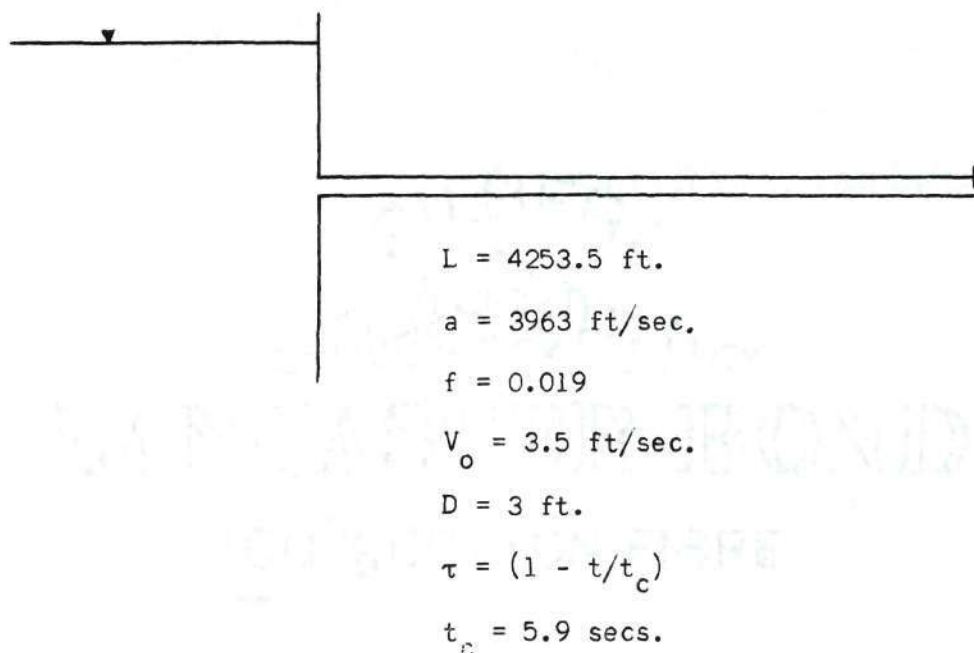


Figure 12. Pipe-Reservoir System.

Initially, the head at the valve is specified as 300 ft. of water. Figure 13 illustrates the variation of this head with time. As illustrated this variation is rather severe, with a difference of almost 200 ft.

between maximum and minimum heads.

Example V

The design of a pumped-storage facility, wherein power is generated during peak demand periods, and the reservoir is refilled during off-peak periods, requires an investigation of surges in the tailrace, both for discharge and pump cycles.

To this end mass and momentum balance equations yield, in a similar manner to Example IV,

$$\frac{dV}{dt} + \sqrt{\frac{gA'}{A}} \frac{dy}{dt} + u \sqrt{\frac{g}{AA'}} \frac{\partial A}{\partial z} \frac{\partial z}{\partial x} + \frac{\tau_o}{\rho R} - gS_o = 0 \quad (114)$$

$$\frac{dx}{dt} = u + \sqrt{\frac{gA'}{A}} \quad (115)$$

$$\frac{dV}{dt} - \sqrt{\frac{gA'}{A}} \frac{dy}{dt} - u \frac{g}{AA'} \frac{\partial A}{\partial z} \frac{\partial z}{\partial x} + \frac{\tau_o}{\rho R} - gS_o = 0 \quad (116)$$

$$\frac{dx}{dt} = u - \sqrt{\frac{gA'}{A}} \quad (117)$$

Employing backward and forward differences on the above,

$$x_i - x_{i-1} = [V_{i-1} + (g \frac{A'}{A'})_{i-1}^{1/2}] (t_i - t_{i-1}) \quad (118)$$

$$v_i - v_{i-1} + (\frac{gA'}{A})_{i-1}^{1/2} (y_i - y_{i-1}) + [V_{i-1} (\frac{g}{AA'})_{i-1}^{1/2} \frac{\partial A}{\partial z} \frac{\partial z}{\partial x} + \frac{\tau_o}{\rho R} - gS_o]_{i-1} \cdot (t_i - t_{i-1}) = 0 \quad (119)$$

$$x_i - x_{i+1} = [V_{i+1} - (g \frac{A'}{A'})_{i+1}^{1/2}] (t_i - t_{i+1}) \quad (120)$$

$$v_i - v_{i+1} - (\frac{gA'}{A})_{i+1}^{1/2} (y_i - y_{i+1}) + [V_{i+1} (\frac{g}{AA'})_{i+1}^{1/2} \frac{\partial A}{\partial z} \frac{\partial z}{\partial x} + \frac{\tau_o}{\rho R} - gS_o]_{i+1} \cdot (t_i - t_{i+1}) = 0 \quad (121)$$

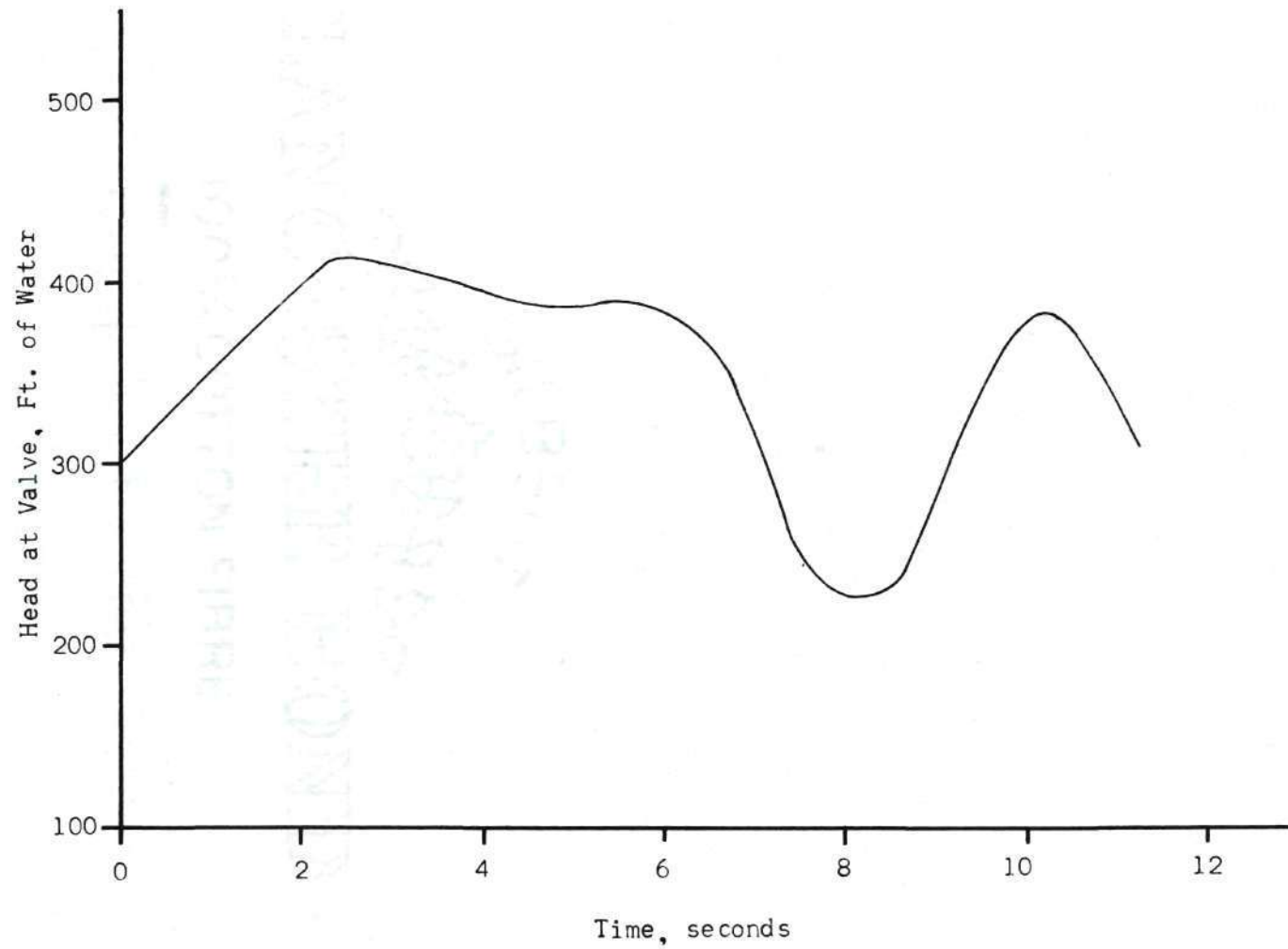


Figure 13. Time Variation of Head at Valve, Example IV.

Similarly to Example IV, these equations may be solved by the assumption of a time step. As an alternative method, it is possible to achieve a simultaneous solution. Such method was programmed for the Univac 1108 computer system. Results follow in Figure 14, illustrating the water depth variation over the pump intake, for times during the starting of the pumps (first 600 seconds) and immediately thereafter.

The examples and equations treated in this section by no means represent the only cases in which difference methods may be used to approximate the solution of a partial differential equation. Sundry variations on the difference techniques also exist, though few of these serve to alleviate the difficulties associated with odd-shaped solution fields, variable material properties, and three-dimensional problems.

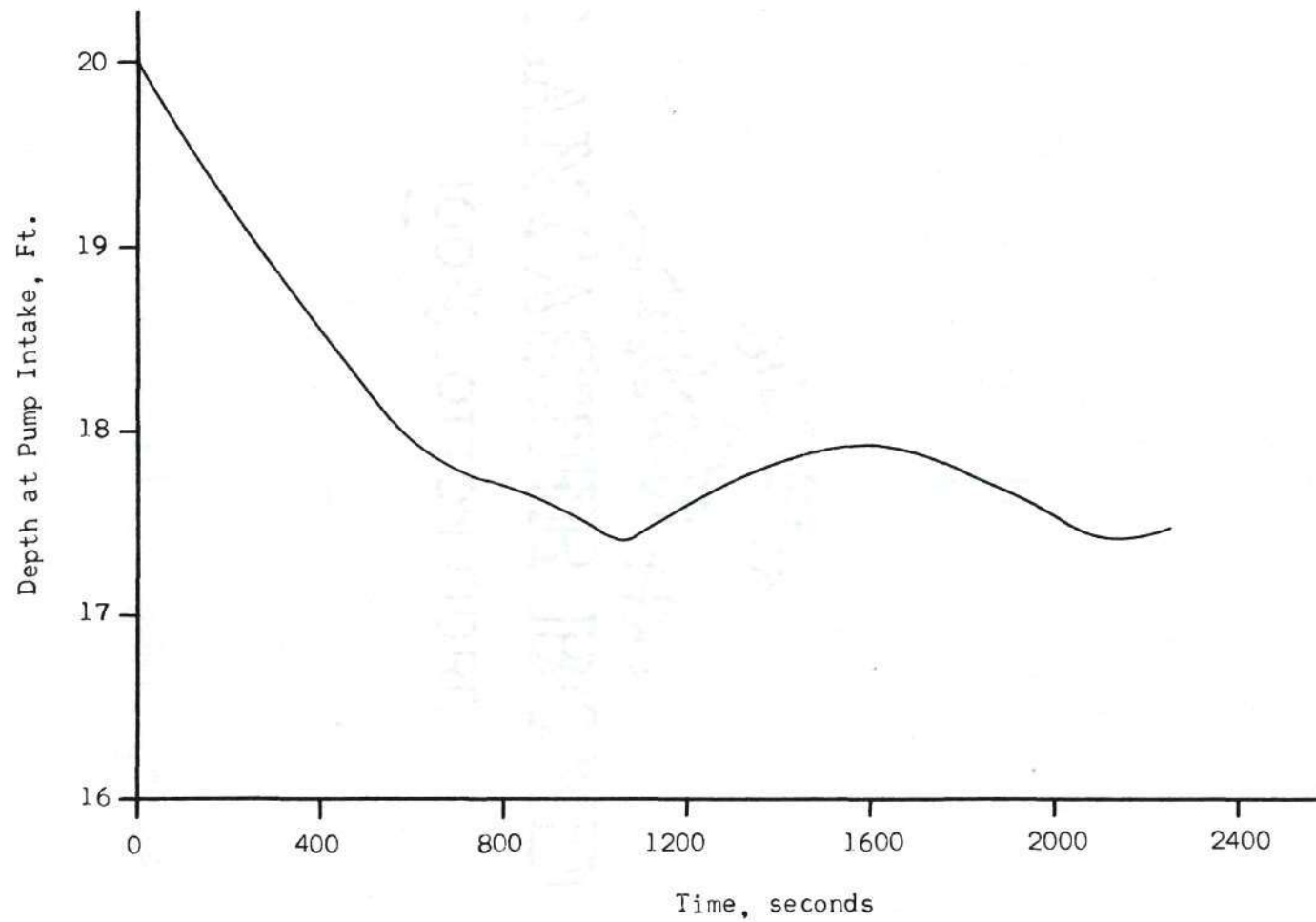


Figure 14. Water Depth over Pump Intake, Using Numerical Model of Example V.

CHAPTER IV

"FINITE ELEMENT" SCHEMES IN PARTIAL DIFFERENTIAL EQUATIONS

In numerous applications, particularly those involving equations of the elliptic type, difference solutions become discouragingly if not impossibly cumbersome. Cognizant of such difficulties with both analytic and difference solutions, Lord Rayleigh suggested in 1870 an alternative method of solution, which involved a variational problem in which the solution function is approximated by a piecewise linear approximation, essentially in the fashion of the final method mentioned in Chapter II. Early in the current century, Walter Ritz generalized upon the method. Today, the Rayleigh-Ritz method has found wide acceptance.

In 1948, Argyris offered an extension to two dimensions, but his formulation was of such complexity that it remained for Clough (8) to popularize the method under the name of the "finite element method." Originally applied to structural analysis, the finite element method found application in various other fields with the formulation (29), (31) of an extension by which field problems might be solved. Such method has been used to date for the solution of problems relating to stress analysis (31), soil and rock mechanics, and of most application here, to seepage problems (30).

Such solution method for field problems requires a different formulation for each type of problem modeled by such scheme. However, once formulated, the model is completely general insofar as boundary conditions,

geometrical and physical properties of the field are concerned. The restriction as to type of problem is of no great concern, as many different phenomena, as well as various applications have a common form insofar as a differential equation model is concerned.

To illustrate how such formulation is developed, an equation of the quasi-harmonic type is considered below.

$$\frac{\partial}{\partial x} (k_x \frac{\partial \phi}{\partial x}) + \frac{\partial}{\partial y} (k_y \frac{\partial \phi}{\partial y}) = f(x,y) \quad (122)$$

This equation is widely used to model such phenomena as the ideal flow of fluids, heat conduction or seepage flows.

Through application of the Euler conditions of the calculus of variations (4), (16) it is shown that a solution of equation (122) also makes the following integral stationary:

$$I = \frac{1}{2} \iint_A \left\{ k_x \left(\frac{\partial \phi}{\partial x} \right)^2 + k_y \left(\frac{\partial \phi}{\partial y} \right)^2 \right\} da - \iint_A f \phi da \quad (123)$$

where A is the area of a discretized portion of the field. In becoming stationary I takes on a minimum. In a physical sense, the principle of minimum energy is satisfied.

At this juncture, it becomes necessary to specify a shape for the discrete elements of the field, and to assume some functional relationship which will adequately describe the solution function within the elements. The basic shape for the discretized subfield is taken to be triangular, as an assembly of such shapes may be most easily used to approximate the geometrical shape of the entire field (Figure 15). Over each subfield, any piecewise differentiable function may be used; though

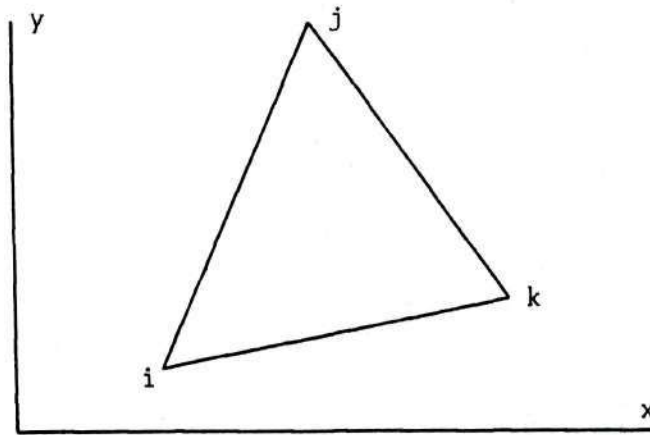


Figure 15. Typical Element.

not requisite for solution here, a linear relation is assumed to hold over each subfield. That is, over each element ijk , it is assumed that

$$\phi = a + bx + cy \quad (124)$$

or equivalently,

$$\phi = \frac{1}{2A} \left\{ (a_i + b_i x + c_i y) \phi_i + (a_j + b_j x + c_j y) \phi_j + (a_k + b_k x + c_k y) \phi_k \right\} \quad (125)$$

where

$$a_i = y_k x_j - y_j x_k \quad (126)$$

$$b_i = y_k - y_j, \quad i, j, k = 1, 2, 3, \text{ in even permutation}$$

$$c_i = x_j - x_k$$

To simplify resulting expressions, matrix notation is used, as

$$\varphi = [N_i, N_j, N_k] \{\varphi^E\} \quad (127)$$

where

$$N_i = \frac{1}{2A} (a_i + b_i x + c_i y), \text{ etc.}$$

Now that an expression for the solution form has been determined, it must be subjected to the condition (123), that

$$\left\{ \frac{\partial I}{\partial \varphi^E} \right\} = \left\{ \begin{array}{c} \frac{\partial I}{\partial \varphi_i} \\ \frac{\partial I}{\partial \varphi_j} \\ \frac{\partial I}{\partial \varphi_k} \end{array} \right\} = 0. \quad (128)$$

Thus,

$$\frac{\partial I}{\partial \varphi_i} = \iint_A (k_x \frac{\partial \varphi}{\partial x} \frac{\partial}{\partial \varphi_i} \frac{\partial \varphi}{\partial x} + k_y \frac{\partial \varphi}{\partial y} \frac{\partial}{\partial \varphi_i} \frac{\partial \varphi}{\partial y}) da - \iint_A f \frac{\partial \varphi}{\partial \varphi_i} da$$

$$\frac{\partial I}{\partial \varphi_j} = \iint_A (k_x \frac{\partial \varphi}{\partial x} \frac{\partial}{\partial \varphi_j} \frac{\partial \varphi}{\partial x} + k_y \frac{\partial \varphi}{\partial y} \frac{\partial}{\partial \varphi_j} \frac{\partial \varphi}{\partial y}) da - \iint_A f \frac{\partial \varphi}{\partial \varphi_j} da \quad (129)$$

$$\frac{\partial I}{\partial \varphi_k} = \iint_A (k_x \frac{\partial \varphi}{\partial x} \frac{\partial}{\partial \varphi_k} \frac{\partial \varphi}{\partial x} + k_y \frac{\partial \varphi}{\partial y} \frac{\partial}{\partial \varphi_k} \frac{\partial \varphi}{\partial y}) da - \iint_A f \frac{\partial \varphi}{\partial \varphi_k} da$$

Substituting from equation (127) and using matrix notation to simplify the expression,

$$\frac{\partial I}{\partial \Phi_E} = k_x \iint_A \begin{bmatrix} \frac{\partial N_i}{\partial x} & 0 & 0 \\ 0 & \frac{\partial N_j}{\partial x} & 0 \\ 0 & 0 & \frac{\partial N_k}{\partial x} \end{bmatrix} \begin{bmatrix} \frac{\partial N_i}{\partial x} & \frac{\partial N_j}{\partial x} & \frac{\partial N_k}{\partial x} \\ \frac{\partial N_i}{\partial x} & \frac{\partial N_j}{\partial x} & \frac{\partial N_k}{\partial x} \\ \frac{\partial N_i}{\partial x} & \frac{\partial N_j}{\partial x} & \frac{\partial N_k}{\partial x} \end{bmatrix} \begin{Bmatrix} \varphi_i \\ \varphi_j \\ \varphi_k \end{Bmatrix} da + \quad (130)$$

$$+ k_y \iint_A \begin{bmatrix} \frac{\partial N_i}{\partial y} & 0 & 0 \\ 0 & \frac{\partial N_j}{\partial y} & 0 \\ 0 & 0 & \frac{\partial N_k}{\partial y} \end{bmatrix} \begin{bmatrix} \frac{\partial N_i}{\partial x} & \frac{\partial N_j}{\partial y} & \frac{\partial N_k}{\partial y} \\ \frac{\partial N_i}{\partial x} & \frac{\partial N_j}{\partial y} & \frac{\partial N_k}{\partial y} \\ \frac{\partial N_i}{\partial x} & \frac{\partial N_j}{\partial y} & \frac{\partial N_k}{\partial y} \end{bmatrix} \begin{Bmatrix} \varphi_i \\ \varphi_j \\ \varphi_k \end{Bmatrix} da + \iint_A f \begin{Bmatrix} N_i \\ N_j \\ N_k \end{Bmatrix} da$$

From equation (126), it is obvious that

$$\frac{\partial N_i}{\partial x} = \frac{b_i}{2A} ; \frac{\partial N_j}{\partial x} = \frac{b_j}{2A} ; \frac{\partial N_k}{\partial x} = \frac{b_k}{2A} \quad (131)$$

and

$$\frac{\partial N_i}{\partial y} = \frac{c_i}{2A} ; \frac{\partial N_j}{\partial y} = \frac{c_j}{2A} ; \frac{\partial N_k}{\partial y} = \frac{c_k}{2A} \quad (132)$$

Substituting into Equation (133)

$$\frac{\partial I}{\partial \Phi_E} = \frac{1}{4A^2} \begin{bmatrix} k_x b_i b_i + k_y c_i c_i & k_x b_i b_j + k_y c_i c_j & k_x b_i b_k + k_y c_i c_k \\ & k_x b_j b_j + k_y c_j c_j & k_x b_j b_k + k_y c_j c_k \\ \text{symmetric} & & k_x b_k b_k + k_y c_k c_k \end{bmatrix} \cdot \iint_A da \begin{Bmatrix} \varphi_i \\ \varphi_j \\ \varphi_k \end{Bmatrix} - \frac{1}{3} f \iint_A da = 0 \quad (133)$$

or,

$$\left\{ \frac{\partial I}{\partial \phi} \right\}^E = \frac{1}{4A} \begin{bmatrix} k_x b_i b_i + k_y c_i c_i & k_x b_i b_j + k_y c_i c_j & k_x b_i b_k + k_y c_i c_k \\ & k_x b_j b_j + k_y c_j c_j & k_x b_j b_k + k_y c_j c_k \\ \text{symmetric} & & k_x b_k b_k + k_y c_k c_k \end{bmatrix} \begin{Bmatrix} \phi_i \\ \phi_j \\ \phi_k \end{Bmatrix} - \frac{A}{3} \begin{Bmatrix} f \\ f \\ f \end{Bmatrix} = 0 . \quad (134)$$

When each triangular element is treated according to equation (134) element may be combined linearly to form a system

$$[S] \{ \phi \} = \{ F \} . \quad (135)$$

Upon application of appropriate boundary conditions, the system described by equation (135) may be solved using any of several methods of computational linear algebra.

Boundary conditions are specified in either of two ways: as given values of ϕ along a boundary or as a normal gradient. Of these, the former is the easier to treat - the known values of ϕ are merely inserted in all pertinent equations. In many applications "mixed" boundary conditions, i.e., boundary values and normal gradients are specified to determine the problem. The normal derivative, as illustrated in Figure 16 is in actuality treated similarly to the term f in equation (121). With reference to Figure 16, specified normal derivatives, usually on a per-unit-length basis, after being multiplied by half the length of the side over which they are effective, are added to the term of the vector F (equation

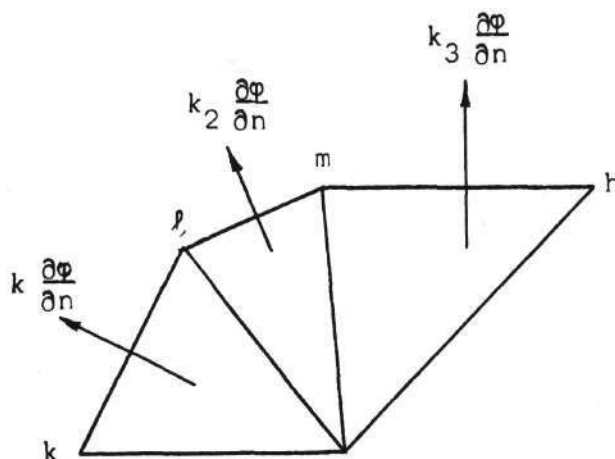


Figure 16. Normal Derivative.

(135)) which describes "loads" on a node. For example, for node m in Figure 16, the term F_m becomes

$$F_m^{(1)} = F_m + k_2 \frac{\partial \phi}{\partial n} \left(\frac{L_{p_m}}{2} \right) + k_3 \frac{\partial \phi}{\partial n} \left(\frac{L_{mh}}{2} \right) \quad (136)$$

It is boundary conditions such as those for ϕ and its gradients that render equation (135) applicable to particular problems. For this reason care in their formulation and application is essential.

Demonstrative applications of such two-dimensional methods are given in Zienkiewicz, Mayer and Cheung (30).

Application of such method to free-surface seepage flows also led to useful results (13),(21),(25). The equation governing such flow is identical to that for enclosed flow through porous media. Only the boundary conditions for the free surface are different. These conditions are (25):

1. Velocity normal to free surface is zero, and
2. Pressure is zero (atmospheric) at the free surface.

Using the finite element approach, the first of these equations is easily satisfied; it is the natural boundary condition for the Rayleigh-Ritz formulation. The second is not as easily applied as an iterative technique is required for solution.

To perform such iteration, an initial free surface is assumed, and pressures are computed throughout the field. The surface is then adjusted so that the second condition is satisfied, and pressures are again computed throughout the field. Such procedure is repeated until pressures are computed to be zero along the free surface. Example VI illustrates this technique.

Example VI

Analysis of the flow of water through porous media may be dependent upon the position of the phreatic surface. The location of this free surface is particularly critical in the design of earth dams and in the planning of construction projects where the water table is quite near the surface.

It is shown variously by the use of the continuity equation and Darcy's law that the heads associated with a flow field through porous media must satisfy

$$\frac{\partial^2 H}{\partial x^2} + \frac{\partial^2 H}{\partial y^2} = 0 \quad (137)$$

In addition, the pressures within the flow field must be such that they are atmospheric along the phreatic surface.

The problem shown in Figure 17 was selected as an example; that of flow between an infinite reservoir and a deep ditch with a flow rate per unit length 0.01 cfs. An analytic solution is known for this problem, and provides a check for the quality of the finite element solution.

To achieve a solution for the location of the free surface, it is necessary to specify an initial solution field, such field being shown partially discretized in Figure 17. A two-dimensional finite element solution is then calculated for this field, and the field is adjusted so that atmospheric pressures indicated by the numerical solution lie along the free surface. The numerical (finite element) solution is then performed for the adjusted field, and the procedure repeated if necessary until atmospheric pressures along the free surface are obtained by the finite element solution. Such convergence is rapid; this example solution required only one adjustment. The final numerical solution, which is accurate to within 0.5 ft is compared with the exact solution in Figure 18.

Related classically as well as physically to the quasi-harmonic equation (122) in Cartesian coordinates is a formulation exhibiting symmetry about an axis. In cylindrical coordinates, equation (122) thus becomes

$$\frac{\partial}{\partial r} \left(k_r \frac{\partial \phi}{\partial r} \right) + \frac{k_r}{r} \frac{\partial \phi}{\partial r} + k_z \frac{\partial \phi}{\partial z} = F(r, z) \quad (138)$$

Again solution may be accomplished by subdivision of the field into finite elements, although rather than area elements, these are elemental volumes, as shown in Figure 19.

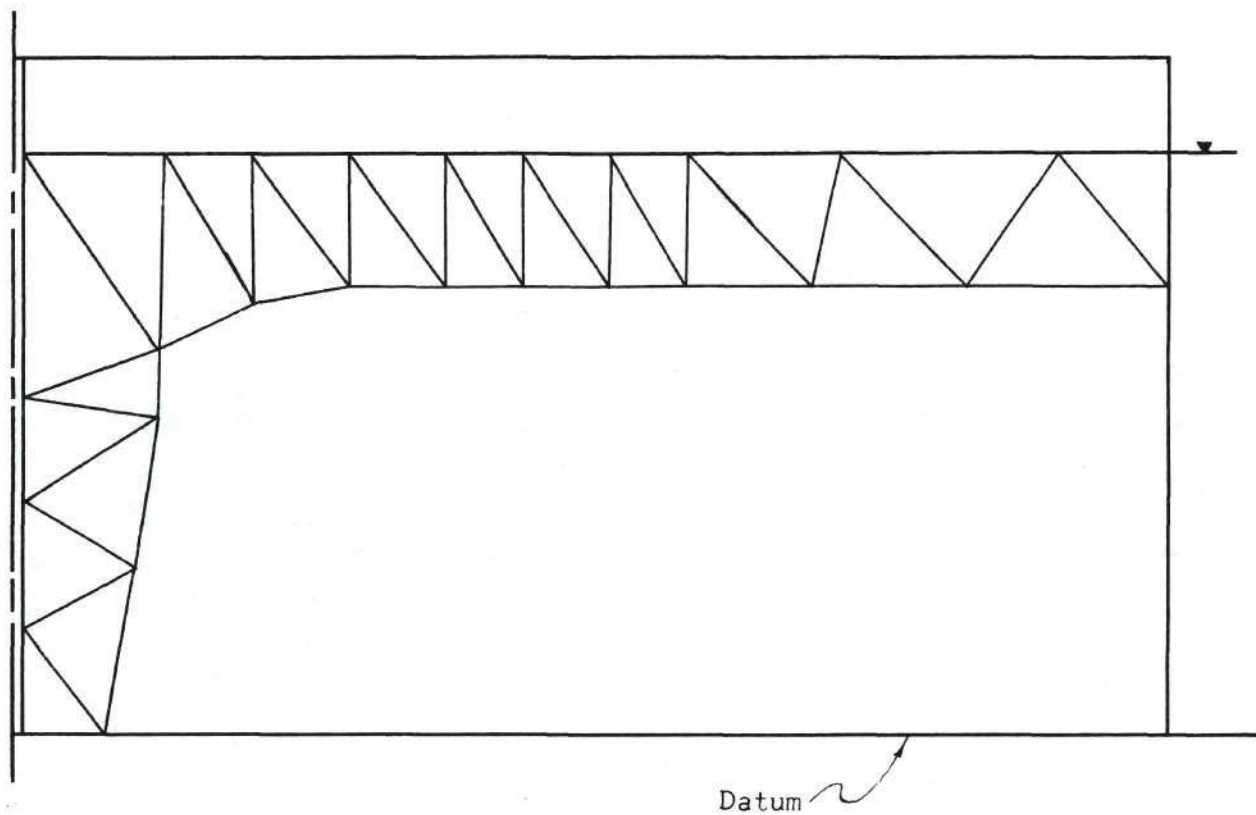


Figure 17. Initial Solution Field for Example VI.

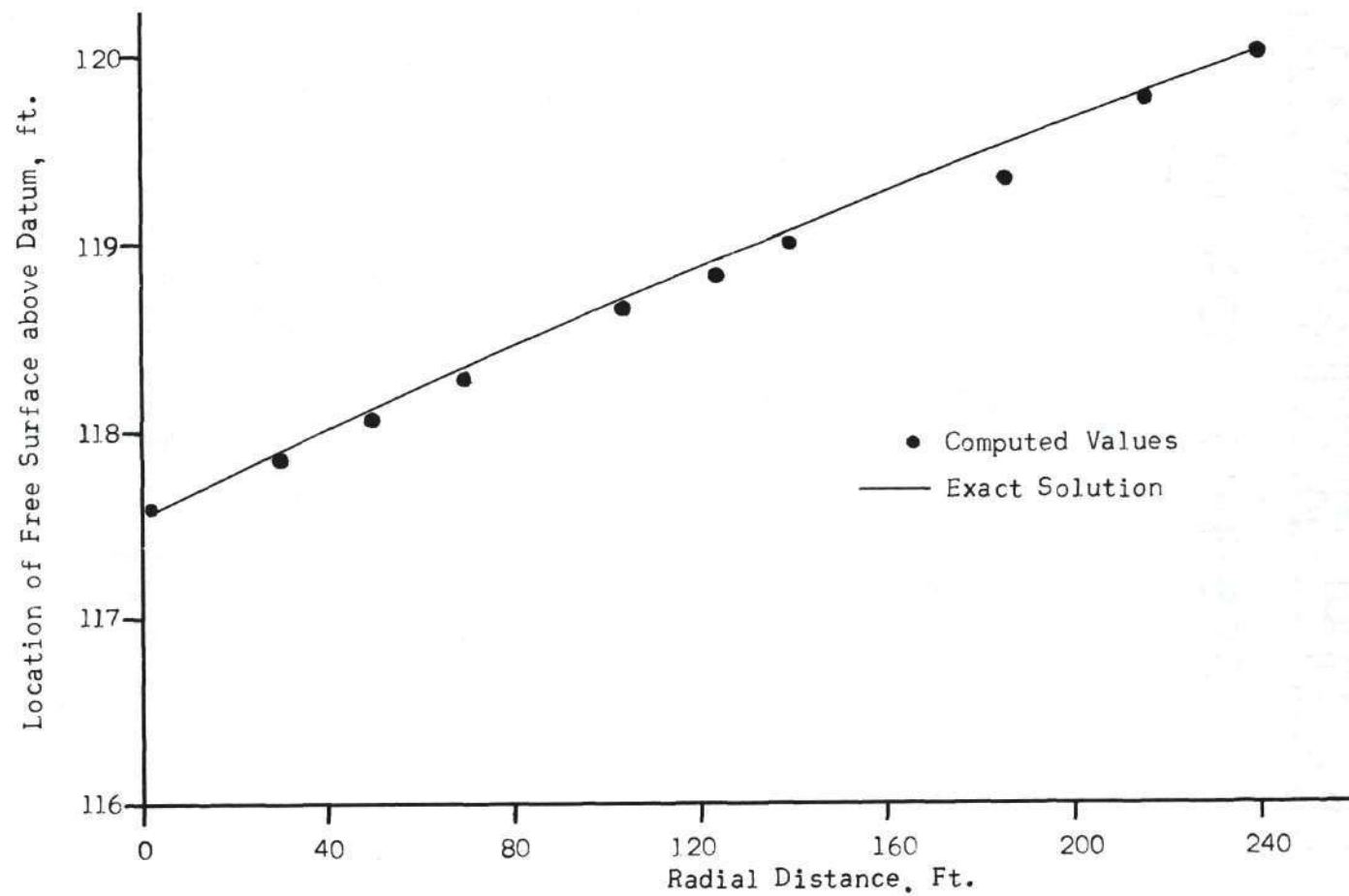


Figure 18. Free Surface as Computed for Example VI.

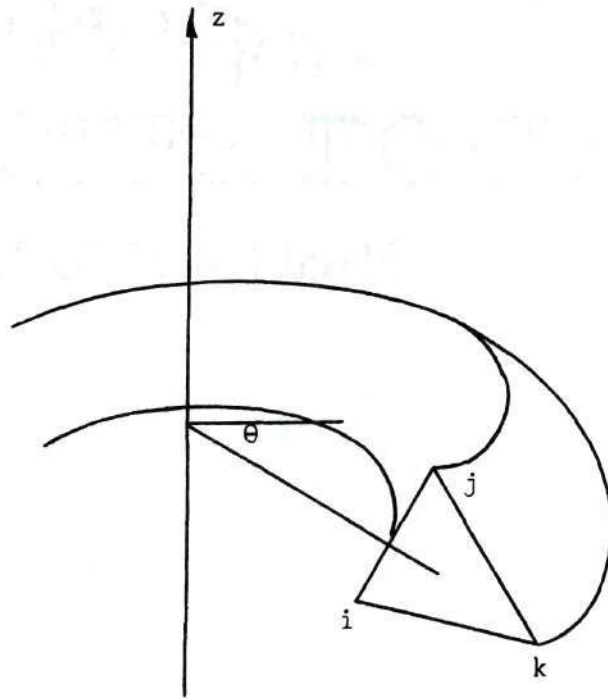


Figure 19. Axisymmetric Volume Element.

Under the assumption that for such an element, ϕ must be linear, the stationary point of the associated functional

$$I_{rz} = 2\pi \iint_A \left\{ -\frac{1}{2} r_k \left(\frac{\partial \phi}{\partial r} \right)^2 + \phi \frac{\partial \phi}{\partial r} - \frac{1}{2} r_k \left(\frac{\partial \phi}{\partial z} \right)^2 \right\} dr dz + \\ + 2\pi \iint_A f \phi dr dz \quad (139)$$

is found. Here r_k , the radial distance to the centroid of the area is used as an approximation to a variable r in the integral.

In a manner similar to that of the two-dimensional finite element formulation, the stationary point

$$\left\{ \frac{\partial I_{rz}}{\partial \varphi_i} \right\} = \left\{ \frac{\partial I_{rz}}{\partial \varphi_j} \right\} = 0 \quad (140)$$

is determined. Thus,

$$\begin{aligned} \frac{\partial I_{rz}}{\partial \varphi_i} &= 2\pi \iint_A \left\{ -k_r r_k \frac{\partial \varphi}{\partial r} \frac{\partial}{\partial \varphi_i} \frac{\partial \varphi}{\partial r} + k_r \frac{\partial}{\partial \varphi_i} \left(\varphi \frac{\partial \varphi}{\partial r} \right) - k_z r_k \frac{\partial \varphi}{\partial z} \frac{\partial}{\partial \varphi_i} \frac{\partial \varphi}{\partial z} \right\} dr dz + \\ &+ 2\pi \iint_A f \frac{\partial \varphi}{\partial \varphi_i} dr dz = 0 \end{aligned} \quad (141)$$

$$\begin{aligned} \frac{\partial I_{rz}}{\partial \varphi_j} &= 2\pi \iint_A \left\{ -k_r r_k \frac{\partial \varphi}{\partial r} \frac{\partial}{\partial \varphi_j} \frac{\partial \varphi}{\partial r} + k_r \frac{\partial}{\partial \varphi_j} \left(\varphi \frac{\partial \varphi}{\partial r} \right) - k_z r_k \frac{\partial \varphi}{\partial z} \frac{\partial}{\partial \varphi_j} \frac{\partial \varphi}{\partial z} \right\} dr dz + \\ &+ 2\pi \iint_A f \frac{\partial \varphi}{\partial \varphi_j} dr dz = 0 \end{aligned} \quad (142)$$

$$\begin{aligned} \frac{\partial I_{rz}}{\partial \varphi_k} &= 2\pi \iint_A \left\{ -k_r r_k \frac{\partial \varphi}{\partial r} \frac{\partial}{\partial \varphi_k} \frac{\partial \varphi}{\partial r} + k_r \frac{\partial}{\partial \varphi_k} \left(\varphi \frac{\partial \varphi}{\partial r} \right) - k_z r_k \frac{\partial \varphi}{\partial z} \frac{\partial}{\partial \varphi_k} \frac{\partial \varphi}{\partial z} \right\} dr dz + \\ &+ \iint_A f \frac{\partial \varphi}{\partial \varphi_k} dr dz = 0 \end{aligned} \quad (143)$$

Stipulation of a linear function φ demands

$$\varphi = N_i \varphi_i + N_j \varphi_j + N_k \varphi_k \quad (144)$$

where

$$\begin{aligned}
N_i &= \frac{1}{2A} [a_i + b_i r + c_i z] \\
N_j &= \frac{1}{2A} [a_j + b_j r + c_j z] \\
N_k &= \frac{1}{2A} [a_k + b_k r + c_k z] .
\end{aligned} \tag{145}$$

Here,

$$\begin{aligned}
a_i &= r_k z_j - r_j z_k \\
b_i &= z_k - z_j \quad i, j, k = 1, 2, 3, \text{ in even permutation.} \\
c_i &= r_j - r_k
\end{aligned}$$

Thus, substituting into equations (141), (142) and (143) and employing matrix notation, it is seen that

$$\begin{aligned}
\begin{Bmatrix} \frac{\partial I_{rz}}{\partial \phi_i} \\ \frac{\partial I_{rz}}{\partial \phi_j} \\ \frac{\partial I_{rz}}{\partial \phi_k} \end{Bmatrix} &= \frac{\pi}{2A} \begin{bmatrix} r_k(b_i b_i + c_i c_i) - (a_i b_i + a_i b_i) & r_k(b_i b_j + c_i c_j) - (a_i b_j + a_j b_i) \\ r_k(b_j b_i + c_j c_i) - (a_j b_i + a_i b_j) & r_k(b_j b_j + c_j c_j) - (a_j b_j + a_j b_j) \\ r_k(b_k b_i + c_k c_i) - (a_k b_i + a_i b_k) & r_k(b_j b_k + c_j c_k) - (a_k b_j + a_j b_k) \end{bmatrix} \\
&\quad \begin{Bmatrix} \phi_i \\ \phi_j \\ \phi_k \end{Bmatrix} - \frac{2\pi A}{3} \begin{Bmatrix} f \\ f \\ f \end{Bmatrix} = 0 \tag{146}
\end{aligned}$$

Equation (146) serves to formulate an expression by which ϕ may be uniquely determined for each elemental volume. Linear combination of such elemental matrices and the introduction of boundary conditions in

similar manner to the two-dimensional case yields a unique solution for the field. Example VII illustrates this application.

Example VII

Common to all transportable quantities, such as mass, heat, vorticity or any of a vast range of quantities is a continuity equation. This common ground gives rise to common solution techniques for flows of heat, mass and similarly transportable quantities.

This example for axisymmetric heat flow is representative of the increasing importance of transport phenomena which play an important role in the design and conception of nuclear facilities, and in efforts related to the exploration of space. A temperature flow field rather than a mass or momentum flow field is the transport phenomenon.

In this example, the temperature distribution in a thick-walled cylinder is sought (Figure 20). Again, an exact solution is known and provides a check on the quality of the finite element solution.

Based upon the steady transport equation for heat and Fourier's law of heat conduction (5), a temperature field must obey the equation

$$\frac{\partial^2 T}{\partial x^2} + \frac{\partial^2 T}{\partial y^2} + \frac{\partial^2 T}{\partial z^2} = 0 \quad (147)$$

In cylindrical coordinates, this is equivalent to

$$\frac{\partial^2 T}{\partial r^2} + \frac{1}{r} \frac{\partial T}{\partial r} + \frac{\partial^2 T}{\partial z^2} = 0 \quad (148)$$

The solution field used for the finite element need only encompass one-half of the cross-section of the cylinder. Symmetry about the axis

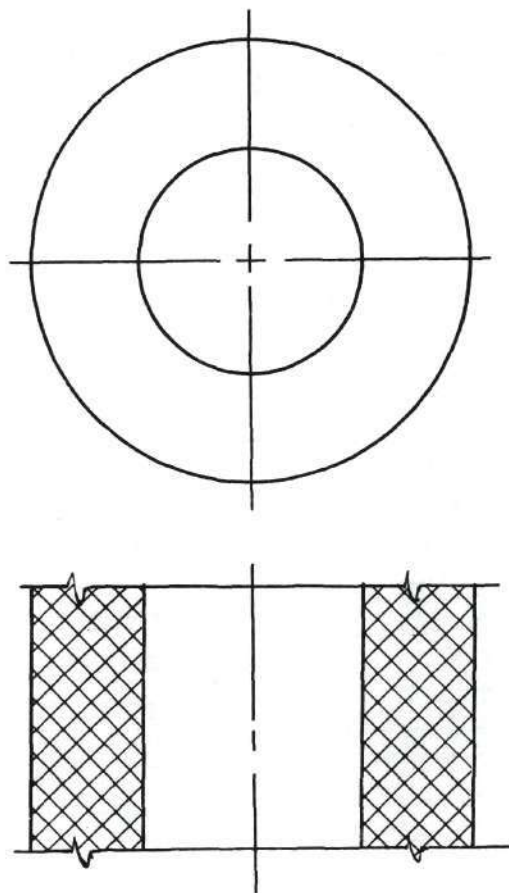


Figure 20. Thick-Walled Cylinder Modelled in Example VII.

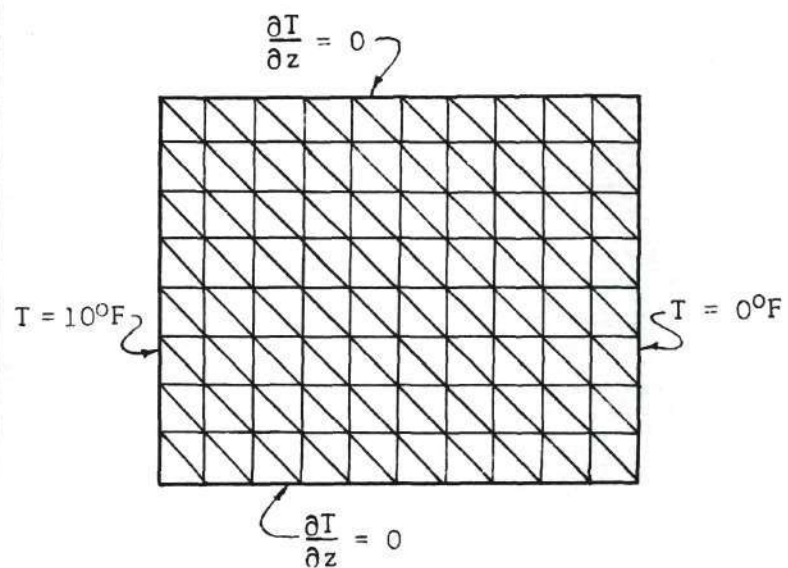


Figure 21. Solution Field for Finite Element Model of Cylinder.

enables the solution to apply to any other cross-section. Such field is shown in Figure 21. The boundary conditions applied are that on the interior surface of the cylinder, the temperature is maintained at a uniform 10°F, and on the exterior surface of the cylinder, a uniform 0°F temperature is maintained.

Subject to these boundary conditions, solutions are presented in Figure 22.

Also related to the quasi-harmonic equation (122) in application is

$$c \frac{\partial \varphi}{\partial t} = \frac{\partial}{\partial x} \left(k_x \frac{\partial \varphi}{\partial x} \right) + \frac{\partial}{\partial y} \left(k_y \frac{\partial \varphi}{\partial y} \right) - Q, \quad (148)$$

which incorporates one form of time-dependence into such problems as those described by the Poisson equation. For purely one-dimensional problems, equations of this sort have been solved through use of differences, as treated above, and to limited extent has been treated by use of the finite element method (28),(29), in two-dimensional fields.

In the context of the finite element development, a Rayleigh-Ritz treatment is used to form the associated functional

$$I_T = \frac{1}{2} \iint_A \left\{ k_x \left(\frac{\partial \varphi}{\partial x} \right)^2 + k_y \left(\frac{\partial \varphi}{\partial y} \right)^2 \right\} da - \iint_A \left\{ Q - c \frac{\partial \varphi}{\partial t} \right\} \varphi da \quad (149)$$

Critical to this development is the assumption that for the spatial portion of the solution, $\frac{\partial \varphi}{\partial t}$ is invariant. To find the solution function φ , a stationary point of the functional I_T must be found. To this end, the solution field is discretized into triangular elements as before, and a linear function

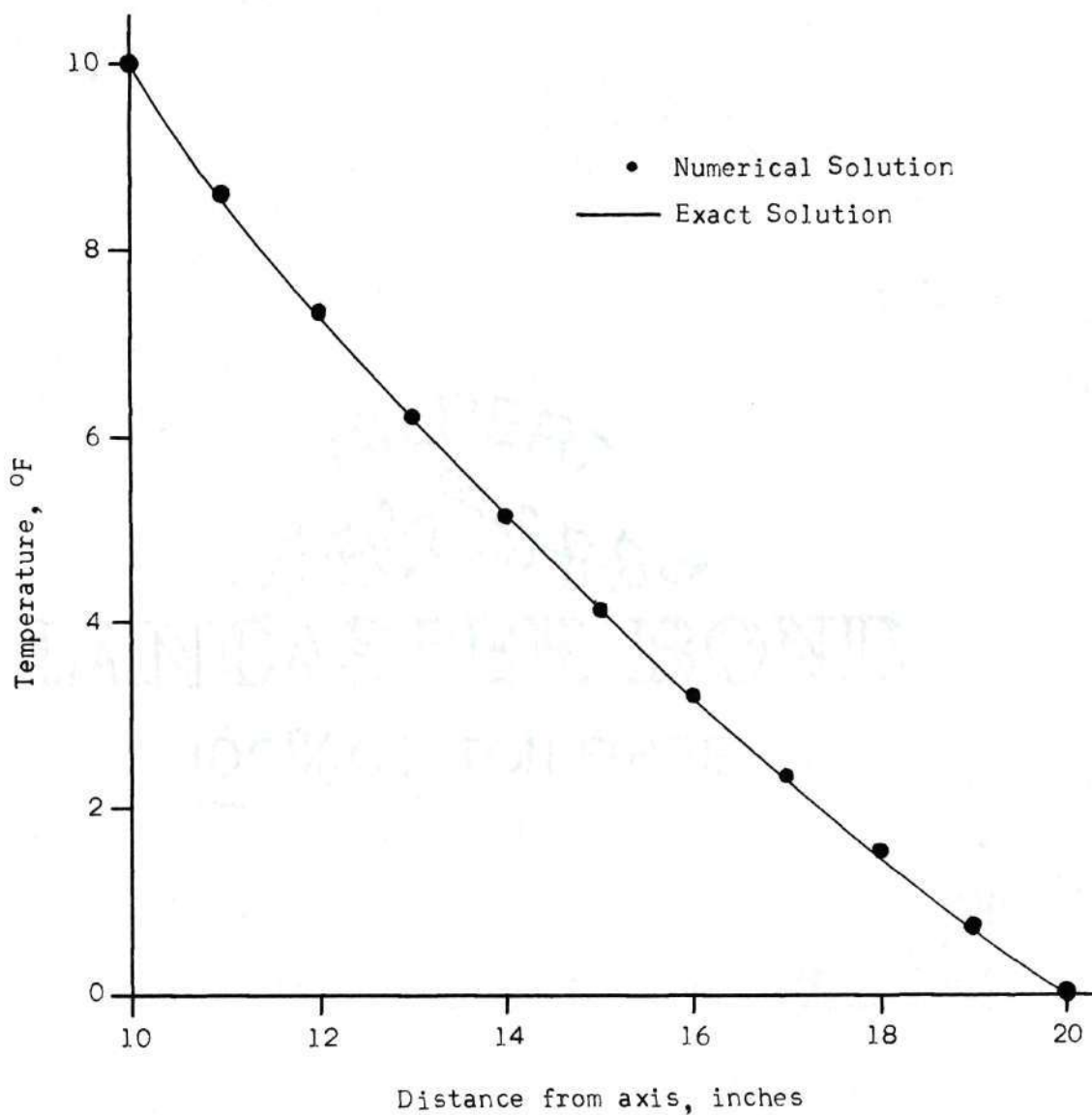


Figure 22. Solution to Axisymmetric Heat Flow Problem (Example VII).

$$\varphi = N_i \varphi_i + N_j \varphi_j + N_k \varphi_k \quad (150)$$

and

$$\frac{\partial \varphi}{\partial t} = N_i \frac{\partial \varphi_i}{\partial t} + N_j \frac{\partial \varphi_j}{\partial t} + N_k \frac{\partial \varphi_k}{\partial t} \quad (151)$$

is assumed to hold over each element. Here, N_i , N_j and N_k are the same as in equations (127). A similar procedure to that for the 2-dimensional case is employed to determine a stationary point for the functional I_T . Indeed, only the term

$$\iint_A c \varphi \frac{\partial \varphi}{\partial t} da \quad (152)$$

is treated differently from the two-dimensional steady-state case.

Treating this term separately,

$$\frac{\partial I_T}{\partial \varphi_i} = c \iint_A \frac{\partial \varphi}{\partial \varphi_i} \frac{\partial \varphi}{\partial t} da \quad (153)$$

$$\frac{\partial I_T}{\partial \varphi_j} = c \iint_A \frac{\partial \varphi}{\partial \varphi_j} \frac{\partial \varphi}{\partial t} da \quad (154)$$

$$\frac{\partial I_T}{\partial \varphi_k} = c \iint_A \frac{\partial \varphi}{\partial \varphi_k} \frac{\partial \varphi}{\partial t} da \quad (155)$$

These equations may be alternatively expressed as

$$\left\{ \frac{\partial I_T}{\partial \varphi^E} \right\} = [P] \left\{ \frac{\partial \varphi}{\partial t}^E \right\} \quad (156)$$

where

$$p_{ij} = c \iint_A N_i N_j \, da \quad (157)$$

or,

$$\begin{aligned} p_{ij} = & \frac{c}{4A} (a_i a_j) + \frac{c}{48A} \{ b_i b_j \sum_{m=1}^3 x_m^2 + (b_i c_j + c_i b_j) \sum_{m=1}^3 x_m y_m + \\ & + c_i c_j \sum_{m=1}^3 y_m^2 \} \end{aligned} \quad (158)$$

Such formulation results in the following system

$$\left\{ \frac{\partial I_T}{\partial \varphi} \right\} = [S] \{ \varphi \} + [P] \left\{ \frac{\partial \varphi}{\partial t} \right\} - \{ F \} = 0 \quad (159)$$

or

$$- [P] \left\{ \frac{\partial \varphi}{\partial t} \right\} = [S] \{ \varphi \} - \{ F \} \quad (160)$$

A step-by-step solution to this system of simultaneous differential equations is then formulated (27), as

$$\{ \varphi |_t \} = \{ \varphi |_{t-\Delta t} \} + \frac{\Delta t}{2} \left\{ \frac{\partial \varphi}{\partial t} |_t \right\} + \left\{ \frac{\partial \varphi}{\partial t} |_{t-\Delta t} \right\} \quad (161)$$

from which

$$\left\{ \frac{\partial \varphi}{\partial t} |_t \right\} = - \left\{ \frac{\partial \varphi}{\partial t} |_{t-\Delta t} \right\} + \frac{2}{\Delta t} (\{ \varphi |_t \} - \{ \varphi |_{t-\Delta t} \}) \quad (162)$$

Premultiplying by $-[P]$,

$$-[P]\left\{\frac{\partial \varphi}{\partial t}\right\}|_t = [P]\left\{\frac{\partial \varphi}{\partial t}\right\}|_{t-\Delta t} - \frac{2}{\Delta t} [P]\{\varphi\}|_t - \{\varphi\}|_{t-\Delta t} \quad (163)$$

By use of equation (160),

$$([S] + \frac{2}{\Delta t} [P])\{\varphi\}|_t = \frac{2}{\Delta t} [P]\{\varphi\}|_{t-\Delta t} + [P]\left\{\frac{\partial \varphi}{\partial t}\right\}|_{t-\Delta t} + \{F\} \quad (164)$$

Use of equations (160) and (164) at each time step thus permits solution for φ and $\frac{\partial \varphi}{\partial t}$ at each node. When used with boundary conditions appropriate to the particular solution sought, a unique solution approximating that to equation (148) is obtained.

Such use is examined in Example VIII.

Example VIII

Transient or time-dependent aspects of transport processes are often intractable by analytic techniques. Nevertheless, they are of considerable importance in that many such problems as encountered in reactive mixtures, heating and cooling of metals, unsteady flow through porous media, or consolidation in soils. These phenomena are all governed by the unsteady transport equations.

This example examines the unsteady heating (or cooling) in a two-dimensional field. The example involves a plate of infinite dimension in the y and z direction and of finite (24") dimension along the x axis. The boundary conditions are initial temperature T_0 and final temperature T_1 . Using the unsteady transport equation and Fourier's law of heat conduction, the temperature field through a portion of this plate is governed by

$$\frac{\partial T}{\partial t} = k \frac{\partial^2 T}{\partial x^2} + k \frac{\partial^2 T}{\partial y^2} \quad (165)$$

where k is the coefficient of heat conduction.

If the following non-dimensional quantities are introduced:

$$\begin{aligned}\theta &= \frac{T_1 - T}{T_1 - T_0} \\ \eta &= \frac{x}{b} \\ \xi &= \frac{y}{b} \\ \tau &= \frac{kt}{b^2}\end{aligned}\tag{166}$$

where b is the half-thickness of the plate, equation (165) becomes

$$\frac{\partial \theta}{\partial \tau} = \frac{\partial^2 \theta}{\partial \eta^2} + \frac{\partial^2 \theta}{\partial \xi^2}\tag{167}$$

A finite element model is then applied to the discretized field shown in Figure 23. As described above, this model incorporates a difference scheme to achieve the time variation; it is inherent in such a scheme that small time steps must be used for satisfactory results. In this example, $\Delta\tau$ was taken to be 0.01.

Solutions for this problem are shown as Figure 24, with a corresponding exact solution superposed on the finite element numerical solution.

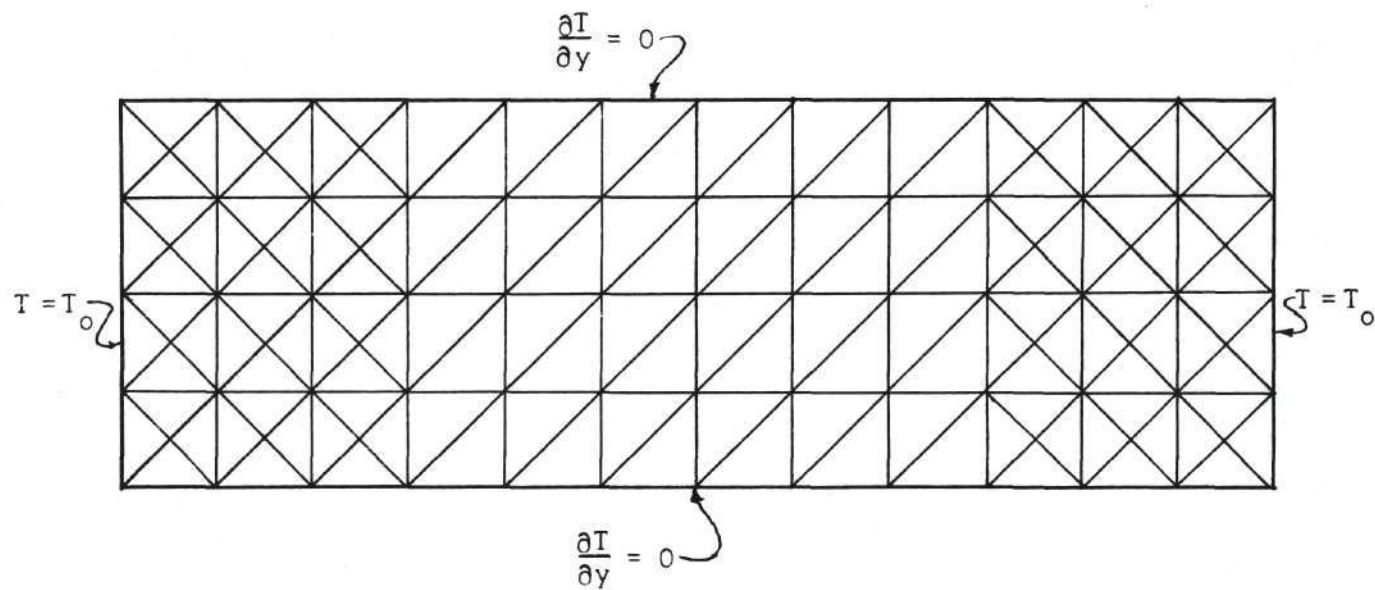


Figure 23. Discretized Field for Solution of Transient Temperatures in a Semi-Infinite Plate.

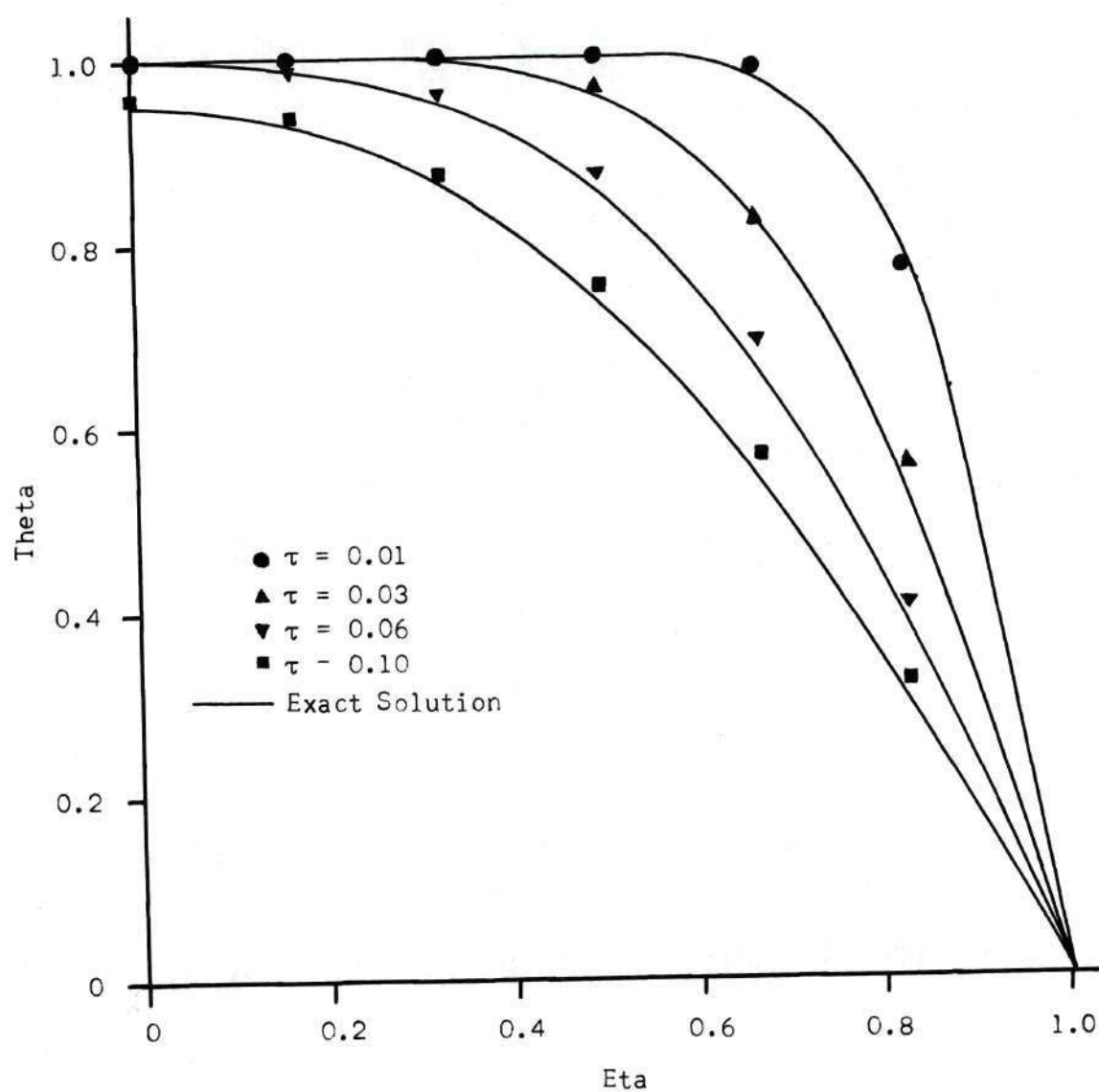


Figure 24. Transient Temperatures in Semi-Infinite Plate (Non-Dimensional).

CHAPTER V

CONCLUSIONS

Numerical modelling in fluid mechanics holds a high promise to provide engineers with powerful and elegant tools by means of which hitherto intractable problems may find satisfactory solutions.

In this thesis, numerical methods were adapted and in part developed in order to solve problems of current interest. Among these problems were those involving time-dependent pipe flows and open channel flows. The problems arose from studies of flows of dilute aqueous high polymer solutions in pipes, from studies of pressure waves in pipes, and from studies of surging in open channels. The methods applied are generally known as those of Runge-Kutta, Adams-Bashforth, and characteristics. The method of characteristics was applied both as the "specified-time-interval" solution (pipe flow) and as the "characteristics grid" solution (open channel).

Southwell's difference schemes were reviewed and presented as the fore-runner of the finite element method. The latter method provides for solutions of problems involving most general geometrical boundary configurations and involving variability of physical properties within the field. Many problems in the field of transport phenomena can be treated. In this thesis, the method has been extended to apply to heat, mass, and momentum transport in the form of

$$\nabla^2 \phi = f(x, y)$$

$$\nabla^2 \phi = f(r, \theta)$$

$$\nabla^2 \phi = c \frac{\partial \phi}{\partial t}$$

Future application of the finite element method will extend to problems of diffusion, convective transport and internal wave effects inherent in fluid flow phenomena. The basic formulation can be readily adapted to particular solution fields while retaining the same general equations.

In summary, this thesis represents an attempt (1) to capsule numerical modelling as an important tool available to engineers and (2) to demonstrate by appropriate examples both the capabilities inherent to numerical methods and the variety of problems that can be treated successfully by the use of high-speed electronic computers

APPENDIX A

NOTATION

A - area

$A' - \partial A / \partial y$

A, B, C, ... matrices when in square brackets

A, B, C, ... column vectors when in braces

D, D_1 , D_2 , ... diameter

F, F_1 , F_2 , ... function

H, H_1 , H_2 , ... head

I - functional

I - identity matrix if in square brackets

K - variable

L, L_1 , L_2 , ... - length

N - variable

N - number of grid points

Q - discharge

Q - constant

R - hydraulic radius

S_o - channel slope

T - function

V - velocity

a, a_1 , a_2 , ... variables

a, b, c, ... column vectors when in braces

a - acceleration
 a - celerity of sound wave
 b, b_1, b_2, \dots variables
 c, c_1, c_2, \dots constants and variables
 f, f_1, f_2, \dots function
 f - Darcy-Weisbach friction factor
 g - gravitational constant
 h - grid size
 i - variable
 j - variable
 k - variable
 k_1, k_2, \dots constants
 l - variable
 m - variable
 n - normal coordinate direction
 n - variable
 r - radial coordinate direction
 r_k - radial distance to element centroid
 S, S_1, S_2, \dots coefficients
 t - variable
 t - time
 u - function
 α - variable
 β - variable
 γ - variable
 Δ - increment

- ϵ - error
- η - variable
- η - transformed coordinate direction
- θ - non-dimensional temperature
- θ - angular coordinate direction
- ξ - variable
- ξ - transformed coordinate direction
- π - constant, 3.1415926...
- ρ - mass density
- τ - variable valve opening
- τ - shear stress
- φ - function

APPENDIX B

REFERENCES

1. Allen, D. N. DeG. Relaxation Methods. McGraw-Hill Book Co., Inc., New York, 1954.
2. Argyris, J. H. "Energy Theorems and Structural Analysis, Part I General Theory," Aircraft Engineering, Vol. 26, October, pp. 137; Nov., pp. 383 (1954); Vol. 28, Feb. pp. 42; March, pp. 80. April, pp. 125, May, pp. 145 (1955).
3. Bennett, A. A., Wm. E. Milne, and Harry Bateman, Numerical Integration of Differential Equations, Dover Publications, New York, 1956.
4. Berg, P. N., "Calculus of Variations," Handbook of Engineering Mechanics, ed. W. Flugge, McGraw-Hill Book Co., Inc., New York, 1962.
5. Bird, R. B., W. E. Stewart and E. N. Lightfoot, Transport Phenomena. John Wiley and Sons, Inc., New York, 1960.
6. Carstens, M. R. and G. D. May, "Seepage Flow Through an Earth Dam," Technical Report 1, OWWR Project B-003-GA, Walter Resources Center, Georgia Institute of Technology, July, 1966.
7. Christian, John T. "Mathematical Preliminaries to the Finite Element Method," Notes, M.I.T. Department of Civil Engineering, Cambridge, Mass., Unpublished.
8. Clough, R. W. "The Finite Element Method in Plane Stress Analysis," Proc. 2nd ASCE Conference on Electronic Computation, Pittsburg, Pa., Sept., 1960.
9. Clough, Ray W., E. L. Wilson and Ian P. King, "Large-Capacity Frame Analysis Programs," Journal of the Structural Division, A.S.C.E., Vol. 89, No. ST4, August 1963, pp. 179-204.
10. Conte, S. D., Elementary Numerical Analysis, McGraw-Hill Book Co., Inc., New York, 1965.
11. Dinnat, R. M. and J. L. Grant, "A Matrix Technique for the Solution of Ordinary Differential Equations," Unpublished.
12. Faddeeva, V. N. Computational Methods of Linear Algebra, Dover Publications, New York, 1959.
13. Finn, W. D. Liam, "Finite Element Analysis of Seepage through Dams," Journal of the Soil Mechanics and Foundations Division, ASCE, Vol. 93, No. SM6, Nov. 1967, pp. 41-48.

14. Hansen, A. G., "Generalized Similarity Analysis of Partial Differential Equations," Nonlinear Partial Differential Equations, Academic Press, Inc., New York, 1967.
15. Hildebrand, F. B., Introduction to Numerical Analysis, McGraw-Hill Book Co. Inc., New York, 1965.
16. Hildebrand, F. B., Methods in Applied Mathematics, Prentice-Hall, Inc., Englewood Cliffs, N. J., 1961.
17. Jeppson, R. W., "Techniques for Solving Free-Streamline, Cavity, Jet and Seepage Problems by Finite Differences," Technical Report No. 68, Department of Civil Engineering, Stanford University, Stanford, California, Sept. 1966.
18. Mayer, P. G., "Unsteady Flow of Dilute Aqueous High-Polymer Solutions in Pipes," OWWR Contract No. B-2561, 1968.
19. McKnown, J. S., En-Yun Hsu and Chi-Shun Yih, "Applications of the Relaxation Method in Fluid Mechanics," Transactions, ASCE, Vol. 120, 1955, pp. 650-686.
20. Olmstead, B. R., Private Communication, 1968.
21. Shamir, Uri, "Flow Through Porous Media by the Finite Element Method," Notes, MIT Department of Civil Engineering, Cambridge, Mass., 1967.
22. Streeter, V. L. and E. B. Wylie, Hydraulic Transients, McGraw-Hill Book Co., Inc., New York, 1967.
23. Southwell, R. V. Relaxation Methods in Engineering Science, Clarendon Press, Oxford, 1940.
24. Southwell, R. V., Relaxation Methods in Theoretical Physics, Oxford University Press, Oxford, 1946.
25. Taylor, R. L. and C. B. Brown, "Darcy Flow Solutions with a Free Surface," Journal of the Hydraulics Division, ASCE, Vol. 93, No. HY2, March 1967, pp. 25-33.
26. Varga, Richard S., Matrix Iterative Analysis, Prentice-Hall, Inc., Englewood Cliffs, N. J., 1962.
27. Wilson, E. L. and Ray W. Clough, "Dynamic Response by Step-by-Step Matrix Analysis," Symposium on the Use of Computers in Civil Engineering, Lisbon, Portugal, 1962.
28. Wilson, E. L. and Robert E. Nickell, "Application of the Finite Element Method to Heat Conduction Analysis," Nuclear Engineering and Design 4, North-Holland Publishing Company, Amsterdam, 1966, pp. 276-286.

29. Zienkiewicz, O. C., The Finite Element Method in Structural and Continuum Mechanics, McGraw-Hill Publishing Co., Ltd. London, 1967.
30. Zienkiewicz, O. C., P. G. Mayer and Y. K. Cheung, "Solution of Anisotropic Seepage by Finite Elements," Journal of the Engineering Mechanics Division, ASCE, Vol. 92, No. EM1, February 1966, pp. 111-120.
31. Zienkiewicz, O. C. and Y. K. Cheung, "Finite Elements in the Solution of Field Problems," The Engineer, Sept. 24, 1965, pp. 507-510.